catalysts

MDPI

Review

Impact of Titanium Dioxide (TiO_2) Modification on Its Application to Pollution Treatment—A Review

Ruixiang Li, Tian Li * and Qixing Zhou *

MOE Key Laboratory of Pollution Processes and Environmental Criteria/Tianjin Key Laboratory of Environmental Remediation and Pollution Control/College of Environmental Science and Engineering, Nankai University, No. 38 Tongyan Road, Jinnan District, Tianjin 300350, China; ruixiangl1998@163.com

* Correspondence: tianli1@nankai.edu.cn; (T.L.); zhouq1x@163.com (Q.Z.); Tel.: +(86)22-58890402; Fax: +(86)22-23501117

Received: 12 July 2020; Accepted: 17 July 2020; Published: 20 July 2020

Abstract: A high-efficiency method to deal with pollutants must be found because environmental problems are becoming more serious. Photocatalytic oxidation technology as the environmentally-friendly treatment method can completely oxidate organic pollutants into pollution-free small-molecule inorganic substances without causing secondary pollution. As a widely used photocatalyst, titanium dioxide (TiO_2) can greatly improve the degradation efficiency of pollutants, but several problems are noted in its practical application. TiO_2 modified by different materials has received extensive attention in the field of photocatalysis because of its excellent physical and chemical properties compared with pure TiO_2. In this review, we discuss the use of different materials for TiO_2 modification, highlighting recent developments in the synthesis and application of TiO_2 composites using different materials. Materials discussed in the article can be divided into nonmetallic and metallic. Mechanisms of how to improve catalytic performance of TiO_2 after modification are discussed, and the future development of modified TiO_2 is prospected.

Keywords: TiO_2; modification; materials; application

1. Introduction

In recent years, photocatalytic technology has attracted extensive attention because it is environmentally friendly, low-cost, and has efficient characteristics. In 1972, Fujishima et al. [1] reported that TiO_2 was used as a photoelectrocatalyst to split water into hydrogen. Since then, increasing research has focused on TiO_2. In 1976, Carey et al. [2] used photocatalytic technology to treat polychlorinated biphenyls, an organic pollution that is difficult to degrade, and experimental results found that the dechlorination rate of polychlorinated biphenyls was close to 100%. In 1977, Frank et al. [3] found that TiO_2 could effectively degrade cyanide (CN^-), which was the beginning of photocatalytic technology applied to pollution control. The degradation of photocatalytic technology can be summarized into four stages: photoexcitation, carrier capture, formation of radicals, and oxidation reaction. Compared with traditional catalytic technologies, photocatalytic technology has many advantages. First, reaction conditions such as sunlight, room temperature, and normal atmospheric pressure are common and easy to obtain. Second, the degradation processes and products of catalytic decomposition are pollution free, which are in line with the requirements of low-carbon environmental protection. Third, the characteristics of non-toxic, stable, low cost, and recyclable further promote development [4]. The core of photocatalytic technology is the photocatalyst, and many materials can act as a photocatalyst [5]. Table 1 shows the published data of different photocatalysts, including TiO_2 [6–8], $SrTiO_3$ [9–11], ZnO [12–14], WO_3 [15–17], ZrO_2 [18–20], and g-C_3N_4 [21–23], and their performance. Among these photocatalysts, TiO_2 occupies an important

position due to its stable physical and chemical properties, strong oxidation capacity, high photocatalytic activity, and excellent biocompatibility [24–26].

The TiO_2 can be synthesized by many methods and mainly include precipitation method, solvothermal method, sol-gel method, microemulsion method, spray pyrolysis method and electrochemical synthesis method. Zhang et al. [27] prepared the TiO_2/BC catalyst material by the sol-gel method and the degradation rates of reactive brilliant blue KN-R in the dyeing wastewater can reach 97%. However, there are still has some problems of pure TiO_2 in application. The rapid recombination of photo-generated electron-hole pairs is the biggest obstacle that affect the practical application of TiO_2 [28], because recombination of photogenerated charge carriers can reduce the overall quantum efficiency [29]. The poor photosensitivity of TiO_2 under visible/solar irradiation is also a problem [30,31]. Generally, the conventional TiO_2 has broad intrinsic band gaps wide band gap (3.2 eV for anatase and 3.0 eV for rutile) which makes the TiO_2 only absorb UV radiation (wavelength < 400 nm), which accounts for only ~5% of the sunlight [32,33]. What is more, nano-TiO_2 is easy to agglomerate, which extremely limits the application. Therefore, in order to solve these problems and improve the catalytic activity of TiO_2 photocatalysts, composites have become mainstream. In addition to the improvement of photocatalysis, composites can yield other benefits. For example, composites can tune the surface properties, i.e., ability to adsorb pollutants. Composites are also beneficial toward the stabilization of nanoparticles against phenomena such as sintering or aggregation [34].

Table 1. The published data of different photocatalysts and their performance.

Type	Photocatalysts	Light Source	Target Pollutant	Degradation Rate	Ref.
TiO_2	$MoS_2/MoO_3/TiO_2$	300 W Xe lamp	rhodamine B	95%	[6]
	Yb, Er, Ce-codoped TiO_2	Xe lamp	4-chlorophenol	95%	[7]
	TiO_2@SiO_2 composites	500 W mercury lamp	methyl orange	99%	[8]
$SrTiO_3$	La- $SrTiO_3$	500 W Xe lamp	Cr^{6+}	84%	[9]
	Ag3PO4/PANI/Cr: SrTiO3	300 W Xe lamp	phenol	99%	[10]
	Ag, Cr-SrTiO3	500 W Xe lamp	methyl orange	98%	[11]
ZnO	Cu-ZnO	blue light lamp	Orange II	70%	[12]
	ZnO	sunlight	methylene blue	90%	[13]
	Sr-ZnO	black light	methylene blue	99%	[14]
WO_3	WO_3	1500 W Xe lamp	N, N-diethyl-meta-toluamide	60%	[15]
	WO_3@Cu@PDI	300 W Xe lamp	tetracycline hydrochloride	85%	[16]
	NiO-WO_3	150 W tungsten lamp	eosin yellow	95%	[17]
ZrO_2	Ce, Er-codoped ZrO_2	halogen lamp	rhodamine B	92%	[18]
	Co_3O_4-ZrO_2	visible light	cyanide	100%	[19]
	Cu- ZrO_2	Visible light	methyl orange	98%	[20]
g-C_3N_4	Ag-P-codoped g-C_3N_4	8 W visible lamps	sulfamethoxazole	99%	[21]

AgI/$LaFeO_3$/g-C_3N_4	500 W Xe lamp	norfloxacin	95%	[22]
CdS/g-C_3N_{42}	500 W Xe lamp	rhodamine B	96%	[23]

The modification of TiO_2 to overcome the problems in the use of pure TiO_2 is one of the widely studied topics in the field of photocatalysis. Modified TiO_2 can improve its photocatalytic activity from different mechanisms, including the reduction of the band gap of TiO_2-based materials, the decrease of the probability of recombination between electron and hole. In recent years, different aspects are applied to improve the photocatalytic efficiency of TiO_2. One of the methods is ion-doped TiO_2 or coupled with other semiconductor composites to reduce the forbidden band width of TiO_2 and increase its absorption wavelength [35–37]. Another way is to deposit precious metals or metal oxides on the surface of TiO_2 and add electron capture agents or use photo-catalysis to prevent TiO_2 photo-generated electron-hole pair recombination thus improve the photocatalytic efficiency of TiO_2 [38–40]. In addition, dye photosensitization and providing a suitable carrier for TiO_2 would be the efficient methods to modify TiO_2 [41].

In recent years, many reviews have been conducted on the modification of TiO_2. Serpone [42] reviewed the different mechanisms of anion- and cation-doping TiO_2. He reported that TiO_2 photocatalysts doped with either anions or cations have recently been shown to have their absorption edge red-shifted to lower energies (longer wavelengths), thus enhancing photonic efficiencies of photoassisted surface redox reactions, and author argued that the red-shift of the absorption edge is due to the formation of color centers. Devi and Kavitha [43] reviewed the photocatalytic activity of non-metal doped TiO_2 for a wide variety of pollutant degradation under UV/visible light, with special emphasis on nitrogen-doped TiO_2. They also discussed the mechanisms of photocatalytic reactions according to the charge carrier generation–separation–transfer–recombination dynamics together with pollutant adsorption and their reactions with reactive oxygenated species in liquid or gaseous regime. Asahi et al. [44] reviewed previous studies on nonmetal-doped TiO_2 for visible-light sensitization. Among the enormous number of studies and references on this topic, they focused on N-doped TiO_2. The present review will concentrate on the application of modified TiO_2 in different media. First, this review summarizes the principles and types of different materials for modifying TiO_2. Then, it discusses the application and progress of modified TiO_2 in treating different pollutants. Finally, it assesses the critical application challenges and potential future research directions.

2. Non-Metallic Materials Modified TiO_2

2.1. Non-Metallic Materials Supported TiO_2

Loading TiO_2 on the carrier can effectively overcome the problems mentioned above [45]. At present, the non-metallic materials commonly used in loading TiO_2 can be divided into non-metallic porous minerals, glasses, carbon materials, and polymer materials.

The treatment of polluted water by porous mineral composites has aroused attention because of the advantages of high specific surface area, strong adsorption characteristics, and the ability of targeted enrichment of pollutants with the development of non-metallic porous minerals. [46]. As shown in Figure 1, TiO_2 loads into the pores or surfaces of mineral materials and then forms the non-metallic porous minerals/nano-TiO_2 composite system, which can solve the problem of the agglomeration of nano-TiO_2 particles. Pollutants can be adsorbed to the surface of nano-TiO_2 through the ion exchange and increase the contact probability of catalysts with pollutants to improve the degradation rate. Hence, porous mineral/nano-TiO_2 composite systems can improve the photodegradation efficiency of nano-TiO_2. Liang et al. [47] used montmorillonite as the matrix to prepare a TiO_2/montmorillonite composite photocatalyst. The results showed that the montmorillonite matrix improved the capacity of optical absorption capacity from 70% to 87% because the visible light absorption ability (390–780 nm) of the composites was enhanced compared with pure TiO_2. Moreover, the ultraviolet light absorption ability of montmorillonite-supported nano-

TiO_2 composites was improved. Therefore, adding montmorillonite carrier enhances the absorbance of visible light and ultraviolet light. Zhu et al. [48] prepared Mn-TiO_2/sepiolite photocatalytic material using the sol-gel method at different calcining temperatures. They found that the degradation rate of emerald dye could reach 98% when the calcining temperature was 400 °C because sepiolite and Mn broaden the spectral response range of TiO_2. Saqib et al. [49] prepared a nano-TiO_2 supported on zeolite using the liquid impregnation method. The experimental results showed that the degradation rate of methylene blue (MB) dye by the loaded material was four times that of pure TiO_2 because zeolite has a UV-visible radiation transparency, which allowed the excitation of light to penetrate into opaque solid powder and reach the substrate molecules present in intraparticles spaces. Zeolite might have substantially enhanced the proximity of organic molecules to the available active sites where the degradation reaction needs to take place.

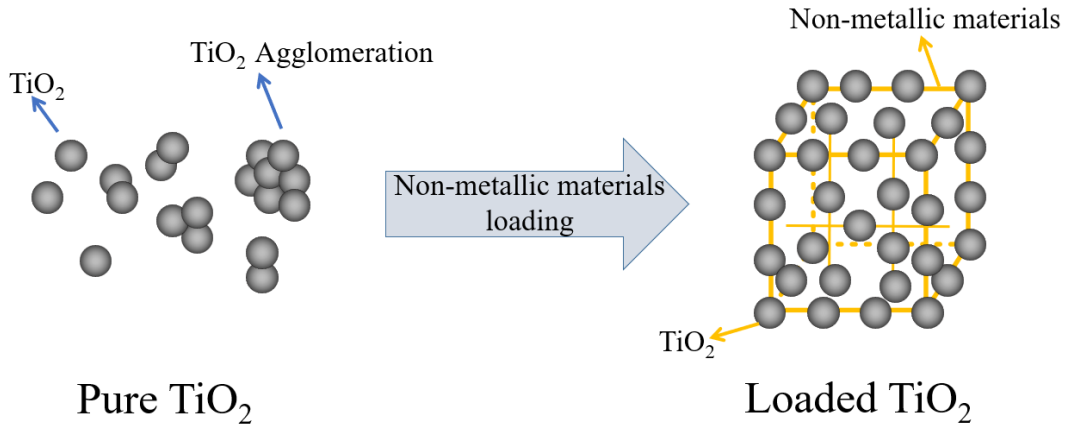

Figure 1. The schematic diagram of non-metallic materials loading TiO_2.

Glass has good light transmission properties and is easy to make into photoreactors with different shapes. Therefore, glass-based carriers have also received widespread attention. The form of glass carrier includes glass sheet, glass tube, glass spring, hollow glass bead, and glass fiber. Malakootian et al. [50] fixed nano-TiO_2 on a glass plate and the removal rate of ciprofloxacin by the composite material reached 93%. Espino-Estévez et al. [51] attached the self-made high-activity TiO_2 to the inner wall of the glass tube reactor by the dipping-lifting method. These results showed that the material had good photocatalytic effect and recycling performance under the ultraviolet light for the degradation of phenol, diclofenac and isoproturon. The degradation rates reached 81% for phenol, 68% for diclofenac and 57% for isoproturon. This was because the decrease of the size of the TiO_2 aggregates The SEM images showed that coatings prepared after milling the TiO_2 suspension were more homogeneous without surface aggregates, which increased the contact area with pollutants. However, the glass surface is relatively smooth, which makes TiO_2 have poor adhesion on it and causes uneven loading of TiO_2.

Combining carbon materials with TiO_2 can substantially improve the photocatalytic activity of TiO_2 mainly because C in the carbon material can effectively promote the separation of photogenerated electrons and holes as an electron trap [52]. Carbon materials include carbon fiber (CF), carbon nitride, activated carbon, carbon nanotubes, and graphene. Chu et al. [53] used the microwave hydrothermal method to load nano-TiO_2 on CF. The experimental results showed that TiO_2/CF has a good photocatalytic activity. The degradation rate of rhodamine B after 1 h of ultraviolet light irradiation reached 95%. When the catalyst was used for 10 cycles, the degradation rate of the dye still reached 88%. They also reported that compared with pure TiO_2 particles, TiO_2/CF was easily recycled when used as a photocatalyst. Nitric acid oxidation treatment of CF generated polar functional groups, which improved the bonding properties between TiO_2 and CF. Hu et al. [54]

prepared 3D flower-like g-C_3N_4/TiO_2 composite spherical materials (FCTCMs) using a simple solvothermal method and studied their photocatalytic performance. The results showed that the photocatalytic performance of FCTCMs under visible light was twice that of FTMs (3D flower-like structure of TiO_2 microspheres) because g-C_3N_4 can broaden the photoresponse range and reduce the recombination rate of photogenerated electron–hole pairs. Cunha et al. [55] prepared TiO_2/activated carbon composites (TiO_2/AC), and the degradation rate of benzodiazapine drugs reached 98% mainly due to the sorption capacity of activated carbons. Thus, pollutants tend to be adsorbed more efficiently on the surface of the composite close to the TiO_2 catalyst. Moreover, TiO_2/AC composites enhance the generation of superoxide radicals and hydroxyl radicals.

Titanate nanomaterials (especially titanate nanotubes, TNTs) as the carriers of TiO_2 and the adsorbents for heavy metals have attracted great attention from researchers [56]. Because their high specific area, great ion-exchange properties, easy solid–liquid separation and abundant functional groups [57,58]. As the carriers of TiO_2, titanate nanomaterials can provide lots of nano-scale reactive sites when reacting with contaminants and improve the separation between catalysts and pollutants for the good sedimentation property of titanate nanomaterials [31]. Liu et al. [59] synthesized the TiO_2/titanate nanosheet composite material (TNS) and used of Cr(VI) and 4-cholophenol (4-CP) as the target pollutants to tested its performance. The resulted showed that the Cr(VI) removal efficiency attained 99.7% within 120 min and the removal efficiency of 4-CP was 98% within 60 min. They reported that the excellent performance was mainly because the synergetic photocatalysis and autosynchronous doping. The efficiency of the separation between electron-hole pairs was enhanced due to the combination of photo-reduction of Cr(VI) by electrons and photo-degradation of 4-CP by holes. In addition, the adsorption of the reduced Cr(III) by TNS can narrowed energy band gap and enhanced photocatalytic activity of the materials. Zhao et al. [60] constructed the TiO_2 decorated titanate nanotubes composite (TiO_2/TNTs) and used for photocatalytic degradation of bisphenol A (BPA). They compared the performance of the TiO_2, TNTs, and TiO_2/TNTs. The experiment result showed that in the first cycle, the degradation rate of BPA using TiO_2, TNTs, and TiO_2/TNTs was 100%, 5.8%, and 94% under UV light. Although the removal efficiency of BPA by TiO_2 is slightly higher than that of TiO_2/TNTs in the first cycle, reusability of TiO_2/TNTs was proved in the next cycles. After five reuse cycles, the degradation rate of BPA still reached 91% by using TiO_2/TNTs and 95.8% of the material could be separated after 6 h gravity-settling, while the 1.8% BPA was removed and 93% of TiO_2 will lose after gravity settling and cannot be reused in pure TiO_2 group. Besides, Li et al. [61], Cheng et al. [62], and Ji et al. [63] also used titanate materials modified TiO_2 to treated the 4-chlorophenol, phenanthrene, and sulfamethazine, respectively.

In addition, many types of polymer materials have been chosen as catalyst carriers, such as polyethylene (PE), polyvinylidene chloride (PVDF), and polyaniline (PANI) Tu et al. [64] incorporated rectorite (REC) into a porous polycaprolactone (PCL)/TiO_2 nanofiber and tested its photocatalytic performance. The results showed that the degradation rate of PCL/TiO_2/REC to rhodamine B was 98%. Because the porous PCL mats could provide large contact area for TiO_2. Besides, the addition of rectorite (REC) could reduce the diameters of fibers and enlarge the specific surface area, which might improve the photocatalytic efficiency. Ni et al. [65] fixed nano-TiO_2 nanometers in a polyvinyl alcohol–ethylene–ethylene nanofiber scaffold and tested its photocatalytic performance by using methylene blue (MB) as a target pollutant. The experimental results showed that the degradation rate of MB was 97% in 150 min. Mohsenzadeh et al. [66] synthesized the PANI-TiO_2 nanocomposite using the n-situ deposition oxidative polymerization method. The results showed that the material had good photocatalytic degradation performance for 1,2-dichloroethane wastewater because of the large contact area for TiO_2.

Although non-metallic materials loaded TiO_2 can improve the photocatalytic activity, there are still many problems. High-quality carriers and immobilization methods to complete the photocatalyst loading is necessary. Furthermore, the interaction between carriers and photocatalyst and its effect on catalytic efficiency need to be investigated.

2.2. Non-Metal Element Doping Modification

The doping of non-metal elements has always been a hot spot in the field of photocatalytic modification. Doping non-metal atoms can broaden the photoresponse range of TiO_2. Non-metal ion doping reconstructs TiO_2 valence band and moves it upward, which can shorten the gap width (Figure 2).

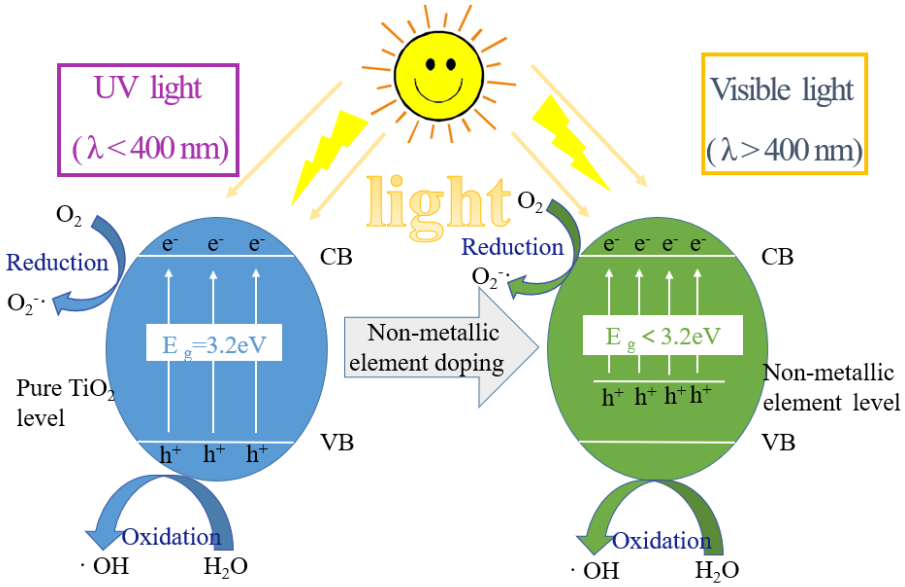

Figure 2. The mechanism of non-metallic element doping modification system.

The lifetime of photogenerated electron-hole pairs and the region of light response to visible light are vital for TiO_2 to increase the value in pollutant treatment [67]. In recent years, it has been found that doping non-metallic elements such as S, N, C, B, I, and F to TiO_2 successfully extended the optical response range of nano-TiO_2 to the visible light region. Non-metal element doping means that oxygen or partial oxygen in the TiO_2 was replaced by non-metals. The new energy band was reconstructed and the width of the forbidden band was shortened during doping the non-metal element [68–70]. As a result, the light response range was expanded. Doping non-metallic elements could increase the impurity level in the forbidden band of TiO_2 and help the band energy level keep higher than the reduction level, where the energy level of TiO_2 are overlap [71–73]. Asahi et al. [74] first replaced a small amount of lattice oxygen in TiO_2 with non-metallic element N doping, and successfully achieved visible light catalytic activity of TiO_2. The preparation method of non-metal element doped TiO_2 photocatalyst can be divided into post-treatment and process treatment. Process treatment means that non-metal elements was doped during the formation of TiO_2, and post-treatment means that non-metal elements was doped after TiO_2 formation.

Li et al. [75] prepared N-doped TiO_2 using the sol-gel method, and the degradation results of dye methylene orange (MO) showed that the degradation rate of pure TiO_2 was less than 5% after 180 min under visible light, whereas that using N-doped TiO_2 as the catalyst was over 95% after 90 min. N doping substantially enhanced the ability of TiO_2 to degrade MO under visible light because N impurity and Ti^{3+} acted cooperatively to narrow the band gap of N-doped TiO_2. Jyothi et al. [76] prepared N and F co-doped TiO_2 using the hydrothermal method to remove bromoethane in the solution. The doping element inhibited the photogenerated electron–hole recombination to generate the hydroxyl radical (•OH). The synergistic effect increased the removal rate of bromoethane for 90 min from 54% of pure TiO_2 to 94%. Rahbar et al. [77] prepared S and N co-doped carbon quantum dots (CQDs)/TiO_2 composites using the hydrothermal method. The degradation rate of acidic AR88

(azo dyes) under visible light irradiation was 54%, which was higher than that of pure TiO_2. They also reported that CQDs allowed the separation of charges due to the electron transport characteristics. In addition, the surface functional group enhanced the photocatalytic activity by providing a higher adsorption capacity on the photocatalyst surface, and pollutant molecules were adsorbed on the photocatalyst surface to promote the photocatalytic reaction. Liu et al. [78] used I-doped TiO_2 (I-TiO_2) material as the electrode of the photoelectrocatalytic method. The experimental results showed that the removal efficiency of diclofenac through modified photoelectrode reached 60%, whereas only 10% was removed using the TiO_2 photoelectrode after 2 h (1.4 V) of visible light. Photoexcited electrons in the conduction band (CB) of TiO_2 can be accepted by the carbon structure due to the high electron storage capacity of carbon materials such as carbon nanotubes. Therefore, the doping of non-metal element not only extends the photocatalytic reaction to visible light, but also improves the photon efficiency of TiO_2 by promoting the separation of charge carriers.

Although doping non-metallic elements improves the visible light response of TiO_2, the band gap width reduces. As a result, the oxidizing ability of the TiO_2 nanocrystalline phase is directly reduced, and the adsorbed substances cannot be completely degraded. Therefore, the development of non-metal doping remains a hot and difficult issue in the field of photocatalysis.

3. Metal Materials Modified TiO_2

Metal materials such as stainless steel, nickel mesh and nickel foam can be used as carriers for TiO_2 to solve the pollutant problems. However, metals are generally expensive and damage the crystal lattice in some respects. Therefore, metals are hardly used as carriers. Since the surface of metal is similar to that of glass, it generally has poor adhesion and is difficult to load. Hence, precious metal deposition and metal ion doping are mostly used to modify TiO_2. At present, the metal materials which are used to modify TiO_2 include transition metals (Cr, Fe, and Cu) [79–81], precious metals (Ag, Au, and Pt) [82–84], and rare earth metals (Ce, La, and Nd) [85–87].

3.1. Precious Metal Materials Deposition

Precious metal materials with a large radius are easy to deposit on the surface of TiO_2 particles and can be used as an effective trap for electrons when a certain amount of precious metals is deposited [88–90]. As shown in Figure 3, electrons can transfer from the surface of TiO_2 with a higher Fermi level to the surface of the precious metal with a lower Fermi level. When the Fermi levels of the two surfaces are the same, the electrons will stop transferring and form a Schottky barrier, which can effectively separate photogenerated electron–hole pairs and improve the photocatalytic activity of TiO_2 [70,91,92]. Moreover, depositing an appropriate amount of precious metals on the surface of TiO_2 can broaden the response range of TiO_2 to sunlight and improve the utilization of solar energy, that is, the mechanism of depositing precious metals on the surface of TiO_2 to improve the photocatalytic efficiency changes the surface properties of TiO_2. As a result, the number of electrons on the surface of TiO_2 is reduced, the separation of photogenerated electron–hole pair is promoted, [93–95] and the photoelectric conversion efficiency is improved. Precious metal deposition can improve photocatalytic performance, but the deposition amount on the metal surface must be controlled within a suitable range. If the deposition amount is very large, the metal may become the center of recombination of electrons and holes, which improves the probability of the electron–hole recombination. Therefore, it is not conducive to photocatalytic degradation [96,97]. Precious metal deposition modification has a high selectivity for photocatalytic degradation of organics [98].

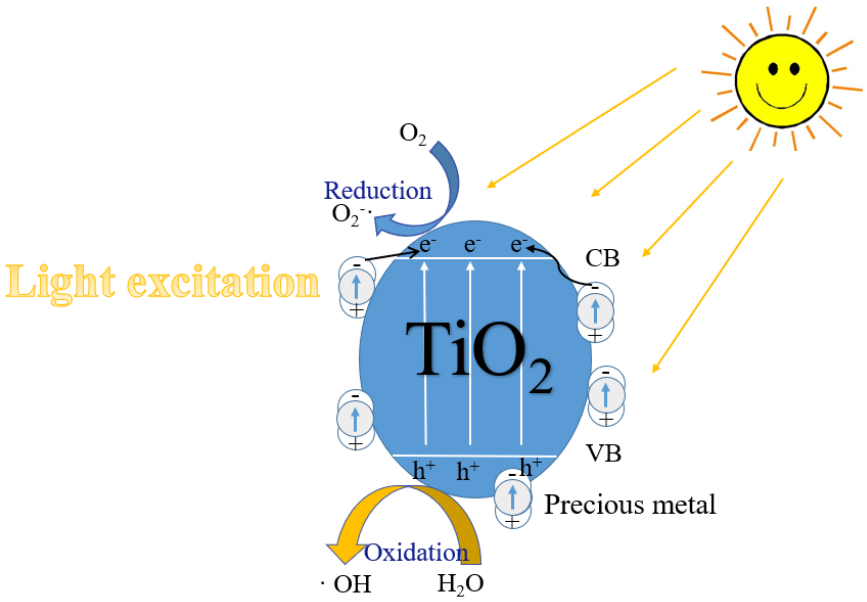

Figure 3. The mechanism of precious metal materials deposition.

In the 1980s, Sato et al. [99] reported that Pt deposited on the surface of TiO_2 enhanced the photocatalytic efficiency of water conversion to H_2 and O_2. Later, Kennedy et al. [100] reported that the incorporation of thermally oxidizable Pt into TiO_2 increased the photocatalytic activity of TiO_2. The oxidation activity of Pt/TiO_2 was higher than the sum of the oxidizing properties of pure Pt and pure TiO_2. The improvement was due to the accumulation of holes at the Pt/TiO_2 interface, which led to a decrease in electron-hole recombination in TiO_2. What is more, the desorption of photo-oxidized intermediated on the surface of TiO_2 and re-adsorption on the surface of Pt with associated thermal oxidation. Ji et al. [101] prepared the Ag-Carbon-TiO_2 composite by using polystyrene/$AgNO_3$ composite fibers as a sacrifice template. They found that the degradation rate of Rhodamine B reached 90%, when the reaction ran 6 h. Shan et al. [102] synthesized biochar-coupled Ag and TiO_2 composites by mixing, calcination, and photodeposition method. They tested the photocatalytic performance of the material by using methyl orange (MO) as target pollutants. The result shows that TiO_2 modified with Ag showed better photocatalytic degradation performance (the highest decolorization efficiency and mineralization efficiency were 97.48% and 85.38%, respectively) than pure TiO_2. They attributed the increase in catalytic efficiency to the promotion of the separation of photogenerated electron hole pairs. Jaafar et al. [103] used in-situ electrochemical method to deposit Ag nanoparticles on the surface of TiO_2 and degraded chlorophenol to measure its photocatalytic activity. The study found that Ag-TiO_2 catalyst degraded chlorophenol to 94% after 6 h, for the electron–hole separation had been enhanced.

The precious metal deposition on the surface of TiO_2 achieves a relatively obvious modification effect that significantly increases the degradation rate of some organic compounds. However, the cost of the precious metal deposition method is very expensive and precious metal deposition modified TiO_2 has a high selectivity for photocatalytic degradation of organics, which further limit the application of these materials in pollution treatment.

3.2. Metal Ion Doping TiO_2

Doping different metal ions in TiO_2 photocatalyst is an effective method to improve its catalytic activity [80,104,105]. Metal ions doped with TiO_2 can change the corresponding energy level structure of TiO_2 because metals are more active, and electrons are more easily excited, resulting in a wider range of the absorption in a TiO_2 system [81,106,107]. As shown in Figure 4, metals can capture the electrons generated by TiO_2 excitation, and the electrons inside TiO_2 are not easy to return to the

original state. After metal doping, metal ions can act as a carrier-trapping center, where metal ions higher than tetravalent are more likely to acquire electrons than titanium ions and metal ions lower than tetravalent trap holes. Ion doping can then stop the recombination of electron–hole pairs, which enables TiO_2 to generate more electrons and holes. Thus, the photocatalytic efficiency of TiO_2 is improved [108,109]. For metals with many valence states, electrons in the d orbitals can transition and enter the TiO_2 lattice, which can reduce the band gap and the energy required for the electron transitions [110,111]. This is vital to improve the activity of TiO_2 photocatalyst [112]. The transition group metal ions doped with TiO_2 can change the crystalline morphology and energy level structure of nano-sized TiO_2 to form impurity energy levels [68]. Photons with lower energy can also undergo transitions, thereby expanding their absorption wavelength range and improving the utilization of visible light [113].

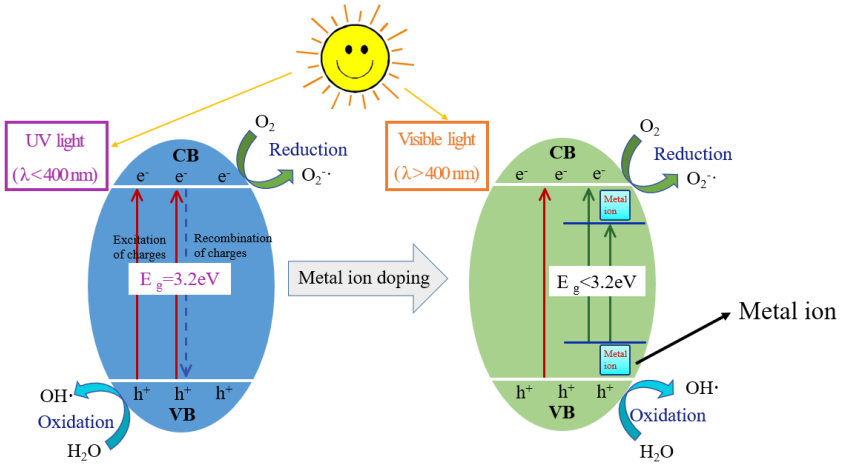

Figure 4. The mechanism of metal ion doping TiO_2.

As early as 1994, Choi et al. [114] began studying the doping of metal ions with TiO_2. In the experiment, 19 kinds of transition metal ions were doped into nano-TiO_2 and showed a better catalytic activity with the dope of Fe^{3+}, Mo^{5+}, Os^{3+}, and Rh^{3+} due to the match of doped ionic potential and radius with TiO_2. Du et al. [115] used Ge^{4+}-doped TiO_2 to prepare Ge/TiO_2 photocatalytic materials and degraded ciprofloxacin. The radius of Ge^{4+} was 0.054 nm, which was smaller than that of Ti^{4+} (0.068 nm). Ge entered the TiO_2 lattice and replaced the position of Ti, causing lattice defects and delaying the recombination of electrons and holes. Therefore, the formation of •OH on the surface of TiO_2 and the photocatalytic efficiency increased. Degradation rate reached 97% when the calcination temperature was 571 °C and the doping amount was 0.26%. Crisan et al. [116] prepared Fe-doped nano-TiO_2 using the sol-gel method, and the absorption spectrum was extended to 546 nm. Moreover, the corresponding band width at the wavelength of 410 nm was 3.03 eV when the Fe content (w) was 2%. Compared with pure TiO_2, the degradation rate of nitrobenzene with 0.5% Fe nano-TiO_2 was increased from 70% to 88%. Gnanasekaran et al. [117] found that the spectral absorption range of Co-doped TiO_2 was extended from 382 to 411 nm when the band gap width was reduced to 3.01 eV. The degradation rate of MO after visible light catalytic treatment for 240 min reached 53%, which was beneficial to its photocatalytic performance. Huang et al. [118] used the sol-gel method to prepare Mo-doped nano-TiO_2 powders, and the degradation rate of MB reached 98% under outdoor sunlight with the amount of 2% Mo^{6+}(w). This result was mainly due to the reduction of the forbidden band from 3.05 to 2.73 eV with the doping of Mo^{6+} and the wider excitation absorption wavelength. Bhatia and Dhir [112] made Ni-TiO_2 and Bi-TiO_2 using the sol-gel method and found that the maximum degradation rate of ibuprofen by Bi-TiO_2 and Ni-TiO_2 reached 89% and 78%, respectively. This finding may be attributed to the increase in specific surface area and the decrease in the crystallite size. Wang et al. [119] prepared an Fe^{3+}-doped TiO_2 nanotube array catalyst using a simple hydrothermal method, which increased the degradation rate of MB by about 20%. The

study also found that Fe^{3+} doping provided traps in the TiO_2 lattice, which greatly improved the separation effect of electron–hole pairs.

4. Composite Materials Modified TiO_2

4.1. The Construction the Heterojunction

The heterojunction is a contact interface, formed as a result of hybridization between two semiconductors [120,121]. The semiconductors used for the heterojunction need to satisfy the condition that they should exhibit different band gaps and the narrow band gap must lie in the visible region [122]. Combining TiO_2 with other semiconductors to construct heterojunction can efficiently improve the photocatalytic performance of TiO_2 [123,124]. This method can not only improve the effective utilization rate of the electrons by promoting the photo-generated electrons and holes to transfer in the opposite direction but also expand the spectral response range of the composite to visible light and even near infrared region [125–127]. Generally, the most widely researched types of the TiO_2-based heterojunction can be categorized into two different types depending on the charge carrier separation mechanism, which are conventional type and direct Z-scheme [128–130].

Based on the different band and electronic structures, the conventional type can be divided in to three, namely, type-I (straddling gap), type-II (staggered gap), and type-III (broken gap) heterojunctions [131,132]. For type-I heterojunctions, the level of the CB of semiconductor-I is higher than that of semiconductor-II, while the valence band (VB) of semiconductor-I is lower than that of semiconductor- II. However, due to the difference between the band gaps, the photoinduced charges accumulate on smaller band gap semiconductor, which may cause recombination. In type-II heterojunctions (Figure 5b), the level of CB and the VB of semiconductor-II are higher than those of semiconductor-I [133]. In addition, the migration of charge carriers to the opposite directions can be promoted because the difference between the chemical potentials causes a phenomenon called band bending. The band structure of the type-III heterojunctions (Figure 5c) is similar to that of type-II except that the staggered gap becomes so wide that the bandgaps do not overlap [134]. Among these conventional heterojunctions, type-II heterojunction attracts the attention of more researchers [135–137]. Ganguly et al. [138] synthesized type-II heterojunctions of the $AgBiS_2$-TiO_2 composite and used doxycycline as the target pollutant to test photocatalytic performance. The results showed that the degradation rate reached 100% in 180 min under a 500 W Xe lamp. The enhanced photocatalytic activity was attributed to the decreased rate of recombination of the photogenerated excitons. Liu et al. [139] used other semiconductors such as Bi_2MoO_6 and TiO_2 to fabricate type-II heterojunctions and tested the photocatalytic performance of Bi_2MoO_6/TiO_2. They reported that the degradation rate of ciprofloxacin, tetracycline, and oxytetracyline reached 88%, 78%, and 78%, within 150 min, respectively, when the 350 W Xe lamp with a 420 nm cutoff filter was used as the light. The CB of TiO_2 can serve as the electron transfer platform, which can improve the efficiency of the separation of photocarriers at Bi_2MoO_6/TiO_2 heterojunction interface.

In 2013, the concept of the direct Z-scheme photocatalyst was first proposed [140]. Figure 5d is the band arrangement and electron migration mechanism of Z-scheme heterojunctions. The Z-scheme heterojunctions have the same band arrangement as the type-Ⅱ heterojunctions, but the electron transfer path between semiconductors is different [141]. The electron transfer path between semiconductors is like the English letter "Z" [142]. In the process of photocatalytic reaction, the photogenerated electrons with lower reduction ability in semiconductor-II recombine with the photogenerated holes in semiconductor-I with lower oxidation ability. Therefore, the photogenerated electrons with high reduction ability in semiconductor-I and the photogenerated holes with high oxidation ability in semiconductor-B can be maintained [143]. In addition, the electrostatic attraction between the photogenerated electron on the CB of the semiconductor-II and the photogenerated holes on the VB of the semiconductor-I will promote the migration of the photogenerated electron from the semiconductor-II to the semiconductor-I, while in the type-II heterojunction, the electrostatic repulsion between the photogenerated electron of the semiconductor-I and the semiconductor-II will inhibit the transfer of electrons from semiconductor-I to the semiconductor-II [144,145]. So far, many

photocatalytic composites that have the Z-scheme heterojunctions have been manufactured to degrade the pollutants. Wang et al. [146] fabricated the N-doped carbon quantum dot (NCDs)/TiO_2 nanosheet with higher surface energy faceted (NCDs/TNS-001) composites and used diclofenac (DCF) as the target pollutants. The photocatalytic efficiency of the composites reached 92% in 60 min under the 350 W Xe lamp. In contrast, only 15.4% of the DCF was degraded in the presence of TNS-001 after 60 min. They reported that the excellent photocatalytic performance might be attributed to the synergistic effects of the highly active facets, up-converted fluorescent properties of NCDs, and efficient charge separation induced by fabricated Z-scheme heterostructures. Hao et al. [147] used the TiO_2@g-C_3N_4 core-shell photocatalysts with the Z-scheme heterojunctions to remove the Rhodamine B from water. The removal efficiency under the 100 Xe lamp was about 96% within 180 min, while the Rhodamine B (RhB) dye shows almost no degradation in the blank test. They attributed the improvement of photocatalytic performance to the formation of the Z-scheme system, which effectively separated photogenerated electrons and holes. Liao et al. [148] prepared a photocatalytic material g-C_3N_4–Ti^{3+}/TiO_2 nanotube arrays and tested its performance of degrading the phenol. At a reaction period of 7 h, the degradation was only 23.4% using TiO_2 nanotube arrays, while the degradation rate increased to 74% using the g-C_3N_4–Ti^{3+}/TiO_2 nanotube arrays. This was mainly because that the self-doping of Ti^{3+} promoted the visible light absorption behavior of the composite and the Z-scheme heterojunctions with efficient space separation of the photo-generated electron–hole.

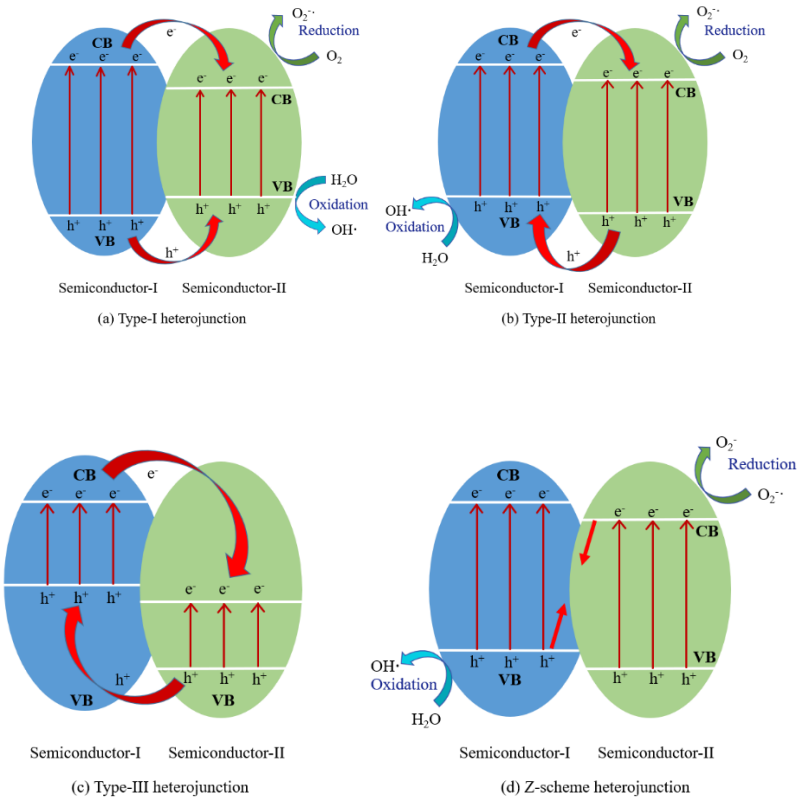

Figure 5. The band arrangement and electron migration mechanism of different heterojunctions. (**a**) Type-I heterojunction; (**b**) Type-II heterojunction; (**c**) Type-III heterojunction; (**d**) Z-scheme heterojunction.

Semiconductor heterojunction powders have exhibited the enhanced photocatalytic activities, but their practical applications have been limited due to their poor recycling performance from flowing wastewater.

4.2. Different Elements Co-Doping TiO_2

The emphasis of single element doping on the modification of TiO_2 is different. In order to improve the migration range of absorption edge, photocatalytic performance and thermal stability of TiO_2 at the same time, the co-doping of multiple elements is an ideal solution [149]. Co-doped nanoparticles exhibit higher visible light absorption than single doped TiO_2 due to a synergistic effect between the two dopants, which can efficiently increase the photocatalytic performance [150]. Co-doping can be divided into different metal elements co-doping [151–153], metal elements and non-metal elements doping [154–156] and different non-metal elements doping [157–159]. As shown in Table 2, many researchers have used co-doping method to modify TiO_2 and tested the photocatalytic performance of the materials.

Table 2. The photocatalytic performance of the co-doped TiO_2 in treating pollutants.

Doping Elements	Crystal Phases of TiO_2	Light Source and Reaction Time	Target Pollutant	Degradation Rate	Ref.
Ni, Cr	anatase	Sunlight 90 min	methylene blue	96%	[153]
Cu, Co	anatase	LED 300 min	acetaldehyde	99%	[160]
Ag, V	-	40 W white light bulbs 180 min	hexane gas butyl acetate gas	94% 96%	[161]
N, Cu	anatase	200 W Xe lamp 60 min	sulfamethoxazole	99%	[162]
Fe, I	anatase	visible light 60 min	gaseous benzene	59%	[80]
Mn, N	anatase, rutile, wurtzite	LED 40 min	Quinalphos 2-chlorophenol	92% 88%	[163]
N, Ag	anatase	LED 360 min	methylene blue	99%	[164]
Ag, Pd, N	anatase	mercury vapor lamp 120 min	malachite green methylene blue mongo red	75% 92% 62%	[165]
C, N	anatase	simulated sunlight 420 min	4-nitrophenol	87%	[166]
N, F	anatase	500 W Xe lamp 150 min	methylene blue	89%	[167]
Si, N	anatase	500 W Xe lamp 180 min	Rhodamine B	86%	[168]
C, N	anatase and rutile	300 W Xe lamp 150 min	phenol	92%	[169]

At present, the physical and chemical properties and the doping mechanism of co-doped TiO_2 with two different metals have not been thoroughly investigated. Singh et al. [170] synthesized the mesoporous La-Na co-doped TiO_2 nanoparticles (NPs). The removal efficiency of MB was almost 100% by using the Na and La doped TiO_2, while 35% MB was degraded by using pure TiO_2 mainly because of the substitution of large-sized Na^{+1} and La^{+3} at Ti^{+4} sites which was confirmed by the results of XRD and TEM. The doping of these low-valent metal ions led to the formation of O vacancies, which promoted the adsorption of hydroxyl groups on the surface of NPs. The adsorbed hydroxyl group reduced the pH_{IEP}, which was beneficial to the adsorption of cationic MB dyes. Metal components prefer to substitute for the Ti site in the TiO_2 lattice to create the dopant level near the CB. Non-metal components can form new levels closest to the VB that reduce the band gap and cause

visible light absorption. Therefore, metal and non-metal ion co-doping enhance photocatalytic activity [163,171]. Garg et al. [172] tested the photocatalytic performance of prepared N and Co-co-doped TiO_2 on the removal of Bisphenol-A under visible light. The results showed that the maximum degradation rate (95%) was observed when using 1.5% Co and 0.5% N co-doping TiO_2. This result was almost twice that of the group using pure TiO_2. TiO_2 was enhanced because Co and N disturbed the physical properties of the nano particles, producing alterations in crystal structure and energy band gap as well as elemental composition. N could easily substitute O in the TiO_2 lattice owing to its atomic size comparable with that of O, and N had small ionization energy and high stability. In addition, the doping of a range of Co could shift the optical absorption edge from UV to visible light range, and Co could behave as recombination centers for the photoinduced charge carriers, thereby decreasing quantum efficiency. Non-metal co-doped TiO_2 have been studied extensively [173–175]. Zeng et al. [176] prepared B/N co-doped TiO_2 photocatalysts and compared their photocatalytic performance with pure TiO_2 under simulated sunlight by using flumequine (FLU) as the target compound. The results showed that the degradation rate of FLU by B/N co-doped TiO_2 was nearly 100%, whereas that of pure TiO_2 was only about 10%. The photocatalytic performance of TiO_2 catalyst was evidently enhanced by B/N co-doping. The relative content of rutile in B/N co-doped TiO_2 catalysts increased with the increase of the B content, which produced a synergistic effect between anatase and rutile. This synergistic effect can be explained by the formation of a semiconductor junction between the anatase phase and the rutile phase, which promoted the separation of photogenerated electrons and holes, thus improving photocatalytic activity.

The method of co-doping can effectively improve the removal efficiency of pollutants by TiO_2. But some of the elements are not suitable for practical use, so it is necessary to find suitable doping materials. And it is essential to find an optimum amount of dopant to increase the separation of charge carriers and prevent the formation of a recombination center.

4.3. Dye Photosensitization

Dye photosensitization means that the photosensitizer (dyes) binds to TiO_2 surface by chemical or physical adsorption, so that the absorption wavelength of visible light shifts to the long wavelength, thus expanding the excitation wavelength response range of TiO_2 and greatly improving the utilization of sunlight [177–179]. The molecule (dyes) absorbing the photon is called as a photosensitizer and the altered material (TiO_2) is the acceptor or substrate [180]. As shown in Figure 6, the mechanism of photosensitization is that once the dyes achieve their excited state by the absorption of photons in the visible range of the solar spectrum, electrons from the dyes' highest occupied molecular orbital (HOMO) are transferred to their lowest unoccupied molecular orbital (LUMO) and subsequently to the conduction band (CB) of TiO_2 [181–183]. In addition, the dyes in solution can be excited to a triplet state under visible light and transfer their excess energy to the O_2. Thus, the electrons in the LUMO react with dissolved oxygen and produce the superoxide anion radical [184]. Dyes used for photosensitization must meet the following characteristics: strong absorption of visible light even the part of the near infrared (NIR) region, photo stability (unless the self-sensitized degradation is required), the existence of some anchoring groups (-SO_3H, -COOH, -H_2PO_3, etc.) and the higher excited state energy than the conduction band (CB) edge of TiO_2 [185,186]. According to the composition, dyes can be divided into two categories: organometallic dyes and organic dyes. Organometallic dyes contain a transition metal in the structure and the organic dyes are composed of organic chromophores [187].

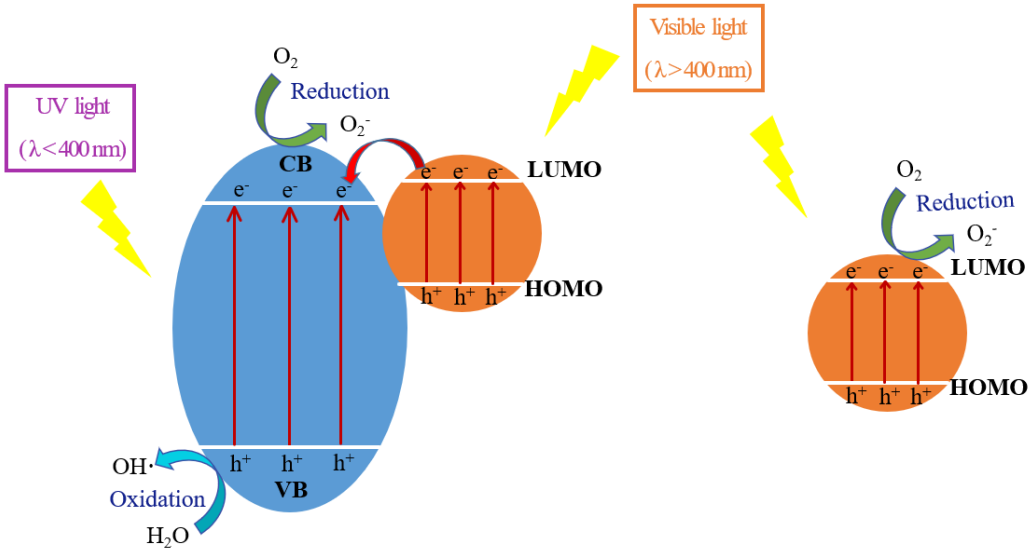

Figure 6. The mechanism of the dye sensitization process.

Ahmad and Kan [188] used a phthalocyanine-based reactive dye, C.I. reactive blue 25 (RB-25), as a dye photosensitizer for anatase (TiO_2) and tested photocatalytic performance by degradation of Rhodamine B (RhB). The result showed that RhB was relatively stable under visible light in the presence of only TiO_2. Degradation rate reached more than 90% when the RB-25 dye was adsorbed on the TiO_2 mainly because the electrons from the dye increased the electron density in the CB of the TiO_2, which enhanced photocatalytic activity under visible light. Mucria et al. [189] modified TiO_2 by dye sensitization. The photosensitizers applied were quinizarin and zinc protoporphyrin. The result showed that the removal efficiency of both exceeded 80%. The improvement of their activity could be ascribed to the presence of sensitizing molecules within the nanotubes, whose electronic properties were promoted by the electron confinement effect in semiconductors. Moreover, electron–hole recombination rate for this material in comparison to the higher surface materials because the electrons can initially reach the dye before the CB. Sensitized materials can also be used for desulphurization. Guo et al. [190] loaded TiO_2 onto SBA-15 molecular sieves and sensitized with organic dyes (2,9dichloroquinacridone, DCQ) to extend its spectral response range from ultraviolet light to visible light. The material was then applied for the photocatalytic oxidation desulfurization of gasoline. Experimental results showed that DCQ-TiO_2@SBA-15 performed better than unsensitized TiO_2@SBA-15, and desulfurization rate can reach 96.1% in a reaction time of 90 min.

The modification method of photosensitization can greatly improve the photocatalytic performance of titanium dioxide. However, there are still some problems need to be solved. For example, the organic dye molecule will gradually degrade due to the photocatalytic. So, it is necessary to replace the catalyst continuously. Additionally, the absorption of most photosensitizers is weak in the near-infrared region and there is adsorption competition with pollutants, which limits the development of photosensitization. Therefore, further research is needed to solve these problems.

5. Application of Modified TiO_2 Composite Photocatalytic Materials

Photocatalytic treatment technology is the most representative advanced oxidation technology for environmental pollution treatment. It uses the hydroxyl radical (•OH) as a strong oxidant to deeply oxidize and decompose organic pollutants into non-toxic inorganic small molecules [191]. At the same time, the photocatalytic reduction reaction can effectively remove heavy metal ions. Table 3 is the performance of the modified TiO_2 in treating pollutants.

Table 3. The performance of the modified TiO_2 in treating pollutants.

Photocatalysts	Crystal Phases of TiO_2	Light Source and Reaction Time	Target Pollutant	Degradation Rate	Ref.
TiO_2/biochar	anatase	500 W mercury lamp 150 min	methyl orange	97%	[192]
Fe^{3+}-TiO_2 nanoparticles	anatase	150 W Xe lamp 240 min	4-chlorophenol ethyl orange	65% 95%	[193]
TiO_2-Fe-porphyrin-conjugated microporous polymers	anatase	Xe lamp 90 min	methyl orange	96%	[194]
Gd-TiO_2	anatase	visible light 93 min	methylene blue	28%	[195]
polypyrrole@TiO_2	anatase and rutile	250 W mercury lamp 60 min	methylene blue	25%	[196]
W, F-TiO_2	anatase	500 W halogen lamp 180 min	methylene blue	96%	[197]
sodium borosilicate glass SiO_2-B_2O_3-Na_2O- ZnO with CdS and TiO_2	anatase	Sunlight 300 min	indigo carmine dye	92%	[198]
TiO_2-$ZrTiO_4$-SiO_2	anatase	300 W Xe lamp 90 min	rhodamine B	95%	[199]
TiO_2-$W_{18}O_{49}$	anatase	visible light 60 min	rhodamine B	82%	[200]
C/Fe-TiO_2 coated on activated carbon	anatase	36 W compact light 140 min	rhoda mine B	99%	[201]
terephthalic acid functionalized g-C_3N_4/TiO_2/Fe_3O_4@SiO_2	anatase	8 W compact fluorescent lamps 120 min	ibuprofen	97%	[202]
Cu-TiO_2	anatase	500 W Xe lamp 140 min	formaldehyde	100%	[203]
MIL-101(Fe)/TiO_2	anatase	Sunlight 30 min	tetracycline	93%	[204]
WO_3/TiO_2	anatase	500 W Xe lamp 60 min	paracetamol	100%	[205]
MoS_2/TiO_2/Carbon Fiber	rutile	visible light 60 min	tetracycline	93%	[206]
Bi2S3/TiO_2/Montmorillonite	anatase	mercury vapor lamp 120 min	ketoprofen	90%	[207]

TiO_2-reduced graphene oxide (TiO_2-rGO)	anatase	simulated sunlight 90 min	formalin	98%	[208]
TiO_2/glass	anatase	Sunlight 30 min	2,5-dichlorophenol	95%	[209]
Bi, B-TiO_2	anatase	Xe lamp 90 min	5-fluorouracil	100%	[210]
Ce, Mn- TiO_2	anatase	30 W ultraviolet lamp 240 min	diclofenac	94%	[211]
Fe-TiO_2	anatase and rutile	visible light 1050 min	acetaldehyde	65%	[212]
N, F-TiO_2	anatase	mercury vapor lamp 180 min	ethylbenzene	33%	[213]
activated carbon-TiO_2	anatase and rutile	UV light 20 min	toluene	99%	[214]
Eosin Y- TiO_2	anatase	visible light 180 min	acetaminophen diclofenac	71% 83%	[185]
Cu-TiO_2 combine with activated carbon fiber	anatase and rutile	fluorescent lamp 180 min	Benzene toluene	81% 98%	[215]

5.1. The Application in Water Pollution

Wastewater treatment plants can remove a large majority of the pollution. However, several trace organic compounds or refractory compounds cannot be degraded by the conventional treatment [216]. These pollutants mostly result from domestic and industrial use of pharmaceutical preparations, printing and hygiene products, and pesticides. In recent years, photocatalytic technology has broadened its application in the treatment of organic wastewater. Under the conditions of sufficient O and light, TiO_2 uses the photogenerated electrons and holes to degrade almost all organic pollutants in water and convert them into CO_2, H_2O, and other inorganic substances. Saif et al. [217] prepared lanthanide (Nd^{3+}, Sm^{3+}, Eu^{3+}, Gd^{3+}, Dy^{3+}, and Er^{3+})-doped TiO_2 using the sol-gel method and evaluated their photocatalytic activity in the treatment of actual sewage. In the actual sewage treatment plant application, the mineralization efficiency of Gd^{3+}-TiO_2 and Eu^{3+} TiO_2 on chemical oxygen demand (COD) reached 67% and 50%, respectively, after 6 h of light. Lima et al. [218] used Ag/TiO_2 photocatalytic material to degrade the hormones which would exist in the sewage treatment plant. The results showed that the degradation rate of the hormone by Ag/TiO_2 reached 95% after 3.5 h. In addition to organic pollutants, photocatalytic technology can achieve better treatment of inorganic substances in water. Peng et al. [219] prepared TiO_2-CuO/HSC composites. Degradation rates of ammonia nitrogen in water reached 61% and 100% when experiments were operated under ordinary light and ultraviolet light, respectively.

Dyeing wastewater discharged from printing and dyeing factories contains a large number of dye molecules. These dye molecules usually contain a mine groups, aromatic rings, azo groups, etc. Therefore, the chromaticity of dye wastewater is difficult to meet standards for discharge. Traditional biological and physical treatment methods for removing organic pollutants, which include precipitation, adsorption, flocculation, reverse osmosis, and ultrafiltration, are inefficient and unsuitable for industrial applications. So, people choose photocatalytic degradation as an alternative technology to solve the pollutants [220–222]. TiO_2 can not only effectively remove the color of wastewater, but also decomposes the pollutants into small molecules such as CO_2 and H_2O. Xu et al.

[223] successfully prepared Ag/TiO_2 layered structure and reported the degradation rate of the dye under the sunlight reached 99%, while the degradation rate of pure TiO_2 was 43%. Ji et al. [224] used C/TiO_2 microsphere to degrade the rhoda mine B. The results showed the degradation rate of rhoda mine B reached 96% within 140 min, and the degradation rate still maintained above 80% after the material was used for three times. Fu et al. [225] use graphene oxide/TiO_2 (GO/TiO_2) composites to degrade the dyes and reported the degradation rate of the dyes reached 96% within 2.5 h.

Tannery wastewater is also a major problem in industrial wastewater because of the containing of large amounts of poorly biodegradable organic chemicals. The general biological treatment method can make the effluent reach the standard, but it still needs multiple treatments to remove most of the COD, color and some organic recalcitrant compounds. So, the photocatalytic treatment using TiO_2 become a new method to treat tannery wastewater. He et al. [226] used Mn-doped TiO_2 material to degrade the tannery wastewater. The degradation rate of organic pollutants under sunlight was nearly 90%. Bordes et al. [227] deposited the fine-structured photocatalytic TiO_2 coatings on austenitic stainless steel coupons by atmospheric plasma spraying (APS) and the total organic carbon (TOC) removal reached 49%, while the decolorization rate reached 75%. Therefore, they reported that the decreased TOC and color removal of the resulting effluent evidenced the effectiveness of the developed coatings for photocatalytic treatment of industrial tannery wastewater.

The large-scale use of pesticides such as herbicides and insecticides have a significant impact on aquatic environment. The harmful effects of these compounds are due to their toxicity and high mobility and persistence in aqueous media [228]. In fact, only a small part of the applied pesticides can protect agricultural products, while most pesticides are lost to the environment through volatilization, hydrolysis, photolysis, or degradation by microbial action [229]. The characteristics of pesticide wastewater lead to ineffective treatment by physical and biological methods, so photocatalytic oxidation is used to treat this type of wastewater, for example organophosphorus pesticides can be mineralized and decomposed by TiO_2 and converted into non-toxic CO_2, H_2O, and PO^{4-}. Abdennouri et al. [230] prepared a nano-TiO_2 supported on pillared clay and found that the material can efficiently degrade 2,4-dichlorophenoxyacetic acid, 2,4-dichlorophenoxypropionic acid, and other pesticides in the environment. Both of the degradation reached about 80%.

As an important component of energy, petroleum plays a decisive role in the sustained and rapid development of the national economy. Due to river convergence and marine accidents, a large amount of low-density and water-insoluble oil flows into the ocean every year, causing marine oil pollution and threating to marine life. Traditional processing is performed by mechanical methods, and biological processes are often used as auxiliary processing steps, followed by advanced processes such as adsorption, membrane filtration, and reverse osmosis. However, due to the presence of high concentrations of toxic aromatic and aliphatic hydrocarbons in addition to the presence of phenols and refractory compounds, the biological processes cannot meet the standard of reuse [231,232]. Studies have shown that TiO_2 photocatalysts can float on the water surface and are efficient in the degradation of toxic and recalcitrant pollutants [233]. Shivaraju et al. [234] prepared N-doped TiO_2. They reported the degradation rate of oil and grease and other organic pollutants in wastewater can reach about 90%.

The pollution of pharmaceuticals in industrial wastewater is serious problem. Traditional wastewater treatment removes most of the pollutants through sedimentation, filtration, adsorption, or biological processes, however, bio-toxic and non-degradable organics usually remain in the water at concentrations above the ppb discharge or reuse limit [235]. Using TiO_2 for photocatalytic reaction would be a good method to solve this problem. Solís-Casados et al. [236] used Sn-doped TiO_2 to treat diclofenac, paracetamol, and ibuprofen under visible light. The results showed the maximum removal rate of diclofenac was 25%, the maximum removal rate of paracetamol was 25%, and the removal rate of ibuprofen was 18%. All of the three drugs were effectively reduced. Malakootian et al. [237] used Fe^{3+} doped TiO_2 materials to degrade pharmaceutical wastewater and antibiotic-added synthetic solutions. The results showed that the degradation rates of antibiotics can reach 70% and 97%, respectively. Besides, Lcerda et al. [238] and Hou et al. [239] also used the TiO_2 to degrade the pharmaceutical wastewater and obtained satisfied result.

5.2. The Application in Air Pollution

Cars provide convenience for people's travel, but the automobile exhaust gas seriously affects air quality and endangers people's health. NO_x in automobile exhaust not only stimulates the human respiratory system, but also causes problems such as acid rain and photochemical smog. So, the removal of NO_x has attracted people's attention. However, the traditional technologies of NO_x removal, including physical adsorption and selective catalytic reduction, cannot remove the NO_x effectively at ppb levels [240,241]. TiO_2 photocatalyst provides an effective way to solve these problems by mixing in paint, concrete and brick or fixing on the surface of roads and walls. Under sunlight, the TiO_2 photocatalyst can oxidize NO_x to form nitric acid through a series of reactions. Then the nitric acid reacts with the components fixed the photocatalyst to obtain nitrate. Under the action of rainwater, nitrate ions are formed and washed away. Zhang et al. [242] found that nano-TiO_2/diatomite composites efficiently degraded formaldehyde in the air, showing a good application prospect. Qin et al. [243] found that loading nano-TiO_2 in concrete during road construction could absorb NO_2 in locomotive exhaust, thereby reducing air pollution.

Besides, most volatile organic compounds (VOCs) in air (aldehydes, ketones and alcohols) are oxidizable, it is feasible to remove them by oxidation method. Most of the heterogeneous catalytic oxidation methods commonly used to remove pollutants in the air at high temperatures, which limits the application. Therefore, the photocatalysis method has become a potential method to remove air pollutants by using water vapor and O_2 in air at room temperature with low energy consumption [244,245]. Lai et al. [246] prepared Bi-TiO_2 to degraded toluene and the degradation rate increased by 77% in terms of CO_2 production, as compared to the pure TiO_2. Rao et al. [247] used Er^{3+} doped TiO_2 and reported the modified TiO_2 exhibited higher photoactivity in comparison with the pure TiO_2. The highest removal efficiency of acetaldehyde and o-xylene within 100 min was 99% and 85%, respectively, and ethylene degradation efficiency reached 22% within 180 min.

5.3. The Application in Soil Pollution

There are many types of soil pollutants, which are characterized by the coexistence of emerging and old pollutants. These pollutants include heavy metals, pesticides, antibiotics, and persistent organic compounds, which makes it difficult to get an efficient repair result in soil. Heavy metal pollution and organic pollution are regarded as the main types of soil pollution because of the large amount among the pollutants [248]. The surface of the contaminated soil with a high concentration of pollutants can easily enter the atmosphere or water under the action of wind and water, respectively, leading to other secondary environmental problems such as air pollution, surface water and groundwater pollution [249–251]. Therefore, soil remediation is imminent.

The pollutants' treatments in soil mainly include physical–chemical remediation technology, biological remediation technology, and phytoremediation technology, but all of these have some shortcomings. The photocatalytic technology can completely mineralize the organic pollutants and remove the heavy metals in the soil. This technology also has the advantages of fast decomposition rate, no secondary pollution, and easy operation [252–254]. In recent years, photocatalysis has been widely used in organic soil remediation studies, including organic pesticides, aromatic organics, petroleum hydrocarbons, and heavy metals [255,256].

TiO_2 is the most widely used catalyst in photocatalyst technology, and it also acts as a key role on pollutants in soil. Kuang et al. [257] reported that the Cd(II) removal efficiency of biological soil crusts increased by 27% than that of pure biological soil crusts after the addition of nano-TiO_2. They reported that in the first 30 min, the adsorption rate of BSC + TiO_2 composite was faster than that of pure TiO_2, which may be due to the high adsorption rate of nano-TiO_2. Petroleum-contaminated soil is highly toxic, and photocatalytic degradation using TiO_2 can also get the ideal results. Yang et al. [258] pretreated the soil with ultraviolet radiation C (UVC) activated TiO_2 under varying moisture conditions to enhance biodegradation of heavy hydrocarbons (HCCs). They reported that total petroleum hydrocarbon (TPH) removal after 24 h exposure to UVC was about 20% in slurries with 300% water holding capacity. In a 10 d bioremediation test, TPH removal in treated soil increased to 27%, compared to 15% for controls without photocatalytic pre-treatment. The improvement mainly

because the recalcitrant hydrocarbons were transformed into more bioavailable and biodegradable products so that the pollutants were more readily consumed by soil microorganisms.

Soil remediation of modified TiO_2 has achieved some effects in heavy metal pollution and organic pollution, but there are still some problems, including the insufficient light penetration and difficulty in recycling. Therefore, it is necessary to find TiO_2 composite materials that can make fuller use of sunlight in the soil or improve the recycling rate.

6. Conclusion and Perspective

Despite the substantial progress in TiO_2, considerable opportunities and challenges remain. The synthesis and improvement of TiO_2 has become a hot topic to improve the efficiency of environmental treatment. This review comprehensively discusses several synthesis and doping technologies of TiO_2, and the effect of each improvement method. Moreover, it elaborates and prospects the application of TiO_2-modified materials in the environmental field, especially for water, air, and soil pollution.

Developing a pollutant treatment with visible light-responsive photocatalysts is very urgent and necessary. The photocatalytic performance of TiO_2 can be greatly improved through the modification of TiO_2. However, many problems in application remain to be solved: (i) in many studies, the system has only one kind of pollutant, which does not match the complex multiple components of the actual pollutants. Gaps exist between material research and application studies for practical application. Whether modified TiO_2 can perform well is unknown. Although modified TiO_2 shows potential in the treatment of pollutants, most of the works considered in the scope of this review were carried out on a laboratory scale. (ii) The recycling or natural degradation of the modified materials remains an issue. Few studies were devoted to separation, recovery, and reuse of photocatalytic materials for the treatment of the real pollutants. (iii) Introduction of other materials into TiO_2 will cause the preparation complexity and cost to increase. Materials used for modification may pollute the environment, such as in modification with heavy metal ions or harmful organic.

Future research should focus on the following aspects to improve the applicability and feasibility of the modified TiO_2: (i) more pilot experiments using modified TiO_2 should be performed for photocatalytic degradation of real pollutants in water, air, and soil. An understanding of inherent charge transfer dynamics and photocatalytic mechanisms at the nanometer and atomic level will be highly useful in designing effective approaches for enhancing the photocatalytic performance of TiO_2. Thus, researchers should understand the mechanism of dealing with actual pollutants. (ii) The efficiency and photostability of the modified TiO_2 must be improved. The performance of modified TiO_2 is currently limited by the physicochemical properties of these materials. (iii) Materials used to modify TiO_2 that cause low harm to the environment and can be used in large patterns must be found or synthesized. Devising an appropriate photocatalyst immobilization strategy to provide a cost-effective solid–liquid separation can save cost and avoid secondary pollution. (iv) A good reactor can improve the utilization rate of light and reduce the electricity costs. Thus, a good design of the reactor is necessary before the experiment. (v) In several cases, toxicity assessment may be even more sensitive than chemical analysis by using modified TiO_2. (vi) Although modified TiO_2 can have a good degradation effect on pollutants in the laboratory, the durability and recyclability of the catalysts must be considered in actual application.

Facing the problems of complex types of pollutants and tight treatment time, the comprehensive application of multiple treatments for pollutants is the development direction of the current environmental field. The combined use of photocatalysis and other technologies will broaden the application of photocatalysis technology.

Author Contributions: R.L. is mainly responsible for the writing of article content and pictures. T.L. modified the article content and pictures. Q.Z. determined the direction of the article.

Funding: This work was financially supported by National Natural Science Foundation of China (21876090), the Tianjin Research Program of Application Foundation and Advanced Technology (18JCZDJC39400 and 19YFZCSF00920), the Postdoctoral Science Foundation of China (2019M660985) and the 111 program of the Ministry of Education of China (T2017002).

Acknowledgments: We acknowledge the use of facilities within the School of Environmental Science and Engineering at Nankai University.

Conflicts of Interest: The authors declare no conflict of interest.

References

1. Fujishima, A.; Honda, K. Electrochemical photolysis of water at a semiconductor electrode. *Nature* **1972**, *238*, 37–38, doi:10.1038/238037a0.
2. Carey, J.H.; Lawrence, J.; Tosine, H.M. Photodechlorination of PCB's in the presence of titanium dioxide in aqueous suspensions. *Bull. Environ. Contam. Toxicol.* **1976**, *16*, 697–701, doi:10.1007/bf01685575.
3. Frank, S.N.; Bard, A.J. Heterogeneous photocatalytic oxidation of cyanide and sulfite in aqueous solutions at semiconductor powders. *J. Phys. Chem.* **1977**, *81*, 1484–1488, doi:10.1021/j100530a011.
4. Xu, M.X.; Wang, Y.H.; Geng, J.F.; Jing, D.W. Photodecomposition of NOx on Ag/TiO_2 composite catalysts in a gas phase reactor. *Chem. Eng. J.* **2017**, *307*, 181–188, doi:10.1016/j.cej.2016.08.080.
5. Karthikeyan, C.; Arunachalam, P.; Ramachandran, K.; Al-Mayouf, A.M.; Karuppuchamy, S. Recent advances in semiconductor metal oxides with enhanced methods for solar photocatalytic applications. *J. Alloy. Compd.* **2020**, *828*, 15, doi:10.1016/j.jallcom.2020.154281.
6. Li, Z.Y.; Cao, F.; Wang, L.; Chen, Z.W.; Ji, X.H. A novel ternary MoS_2/MoO_3/TiO_2 composite for fast photocatalytic degradation of rhodamine B under visible-light irradiation. *New J. Chem.* **2020**, *44*, 537–542.
7. Paeng, D.S.; Huy, B.T.; Phuong, N.T.K.; Dao, V.D.; Lee, Y.I. Photocatalytic activity of Yb, Er, Ce-codoped TiO_2 for degradation of Rhodamine B and 4-chlorophenol. *J. Chem. Technol. Biot.* **2019**.
8. Chen, Y.F.; Tang, X.N.; Zhang, B.; Luo, Y.; Li, Y. TiO_2@SiO_2 Composites: Preparation and Photocatalytic Antimicrobial Performance. *J. Inorg. Mater.* **2019**, *34*, 1325–1333, doi:10.15541/jim20190039.
9. Yang, D.; Zou, X.Y.; Sun, Y.Y.; Tong, Z.W.; Jiang, Z.Y. Fabrication of three-dimensional porous La-doped $SrTiO_3$ microspheres with enhanced visible light catalytic activity for Cr(VI) reduction. *Front Chem. Sci. Eng.* **2018**, *12*, 440–449.
10. Yu, X.; Lin, Y.; Liu, H.; Yang, C.; Peng, Y.; Du, C.; Wu, S.; Li, X.; Zhong, Y. Photocatalytic performances of heterojunction catalysts of silver phosphate modified by PANI and Cr-doped $SrTiO_3$ for organic pollutant removal from high salinity wastewater. *J. Colloid Interface Sci.* **2020**, *561*, 379–395, doi:10.1016/j.jcis.2019.10.123.
11. Zhao, Z.H.; Zhang, X.; Lei, Y.Y.; Yang, P.F.; Fan, J.M.; Zhang, B.; Yin, S. Exceptional photocatalytic activity for Ag,Cr- $SrTiO_3$ activated by H_2O_2 for removal of organic pollutants. *Mater. Res. Express* **2020**, *7*, 10, doi:10.1088/2053-1591/ab6246.
12. Saidani, T.; Zaabat, M.; Aida, M.S.; Boudine, B. Effect of copper doping on the photocatalytic activity of ZnO thin films prepared by sol-gel method. *Superlattices Microstruct* **2015**, *88*, 315–322, doi:10.1016/j.spmi.2015.09.029.
13. Das, A.; Nair, R.G. Effect of aspect ratio on photocatalytic performance of hexagonal ZnO nanorods. *J. Alloy. Compd.* **2020**, *817*, 9, doi:10.1016/j.jallcom.2019.153277.
14. Shkir, M.; Al-Shehri, B.M.; Pachamuthu, M.P.; Khan, A.; Chandekar, K.V.; AlFaify, S.; Hamdy, M.S. A remarkable improvement in photocatalytic activity of ZnO nanoparticles through Sr doping synthesized by one pot flash combustion technique for water treatments. *Colloid Surf. A Physicochem. Eng. Asp.* **2020**, *587*, 9, doi:10.1016/j.colsurfa.2019.124340.
15. Mena, E.; Rey, A.; Rodriguez, E.M.; Beltran, F.J. Reaction mechanism and kinetics of DEET visible light assisted photocatalytic ozonation with WO_3 catalyst. *Appl. Catal. B* **2017**, *202*, 460–472, doi:10.1016/j.apcatb.2016.09.029.
16. Zeng, W.G.; Cai, T.; Liu, Y.T.; Wang, L.L.; Dong, W.Y.; Chen, H.; Xia, X.N. An artificial organic-inorganic Z-scheme photocatalyst WO_3@Cu@PDI supramolecular with excellent visible light absorption and photocatalytic activity. *Chem. Eng. J.* **2020**, *381*, 9, doi:10.1016/j.cej.2019.122691.
17. Rosaline, D.R.; Inbanathan, S.S.R.; Suganthi, A.; Rajarajan, M.; Kavitha, G.; Srinivasan, R.; Hegazy, H.H.; Umar, A.; Algarni, H.; Manikandan, E. Visible-Light Driven Photocatalytic Degradation of Eosin Yellow (EY) Dye Based on NiO-WO_3 Nanoparticles. *J. Nanosci. Nanotechnol.* **2020**, *20*, 924–933, doi:10.1166/jnn.2020.16898.
18. Gionco, C.; Hernandez, S.; Castellino, M.; Gadhi, T.A.; Munoz-Tabares, J.A.; Cerrato, E.; Tagliaferro, A.; Russo, N.; Paganini, M.C. Synthesis and characterization of Ce and Er doped ZrO_2 nanoparticles as solar light driven photocatalysts. *J. Alloy. Compd.* **2019**, *775*, 896–904, doi:10.1016/j.jallcom.2018.10.046.

19. Al-Namshah, K.S.; Mohamed, R.M. Co_3O_4-ZrO_2 nanocomposites: simple preparation and enhanced photocatalytic performance for cyanide degradation under visible light. *Desalin Water Treat* **2019**, *145*, 318–325.
20. Reddy, C.V.; Reddy, I.N.; Ravindranadh, K.; Reddy, K.R.; Shetti, N.P.; Kim, D.; Shim, J.; Aminabhavi, T.M. Copper-doped ZrO_2 nanoparticles as high-performance catalysts for efficient removal of toxic organic pollutants and stable solar water oxidation. *J. Environ. Manag.* **2020**, *260*, 9, doi:10.1016/j.jenvman.2020.110088.
21. Nguyen, T.B.; Huang, C.P.; Doong, R.A.; Chen, C.W.; Dong, C.D. Visible-light photodegradation of sulfamethoxazole (SMX) over Ag-P-codoped g-C_3N_4 (Ag-P@UCN) photocatalyst in water. *Chem. Eng. J.* **2020**, *384*.
22. Zhang, J.J.; Zhu, Z.R.; Jiang, J.C.; Li, H. Fabrication of a novel AgI/$LaFeO_3$/g-C_3N_4 dual Z-scheme photocatalyst with enhanced photocatalytic performance. *Mater. Lett.* **2020**, *262*.
23. Liu, X.M.; Liu, Y.; Zhang, W.K.; Zhong, Q.Y.; Ma, X.Y. In situ self-assembly of 3D hierarchical 2D/2D CdS/g-C_3N_4 hereojunction with excellent photocatalytic performance. *Mater. Sci. Semicon. Proc.* **2020**, *105*.
24. Nalid, N.R.; Majid, A.; Tahir, M.B.; Niaz, N.A.; Khalid, S. Carbonaceous-TiO_2 nanomaterials for photocatalytic degradation of pollutants: A review. *Ceram. Int.* **2017**, *43*, 14552–14571.
25. Hafeez, H.Y.; Lakhera, S.K.; Karthik, P.; Anpo, M.; Neppolian, B. Facile construction of ternary $CuFe_2O_4$-TiO_2 nanocomposite supported reduced graphene oxide (rGO) photocatalysts for the efficient hydrogen production. *Appl. Surf. Sci.* **2018**, *449*, 772–779.
26. Khedr, T.M.; El-Sheikh, S.M.; Ismail, A.A.; Kowalska, E.; Bahnemann, D.W. Photodegradation of Microcystin-LR Using Visible Light-Activated C/N-co-Modified Mesoporous TiO_2 Photocatalyst. *Materials* **2019**, *12*.
27. Zhang, S.C.; Lu, X.J. Treatment of wastewater containing Reactive Brilliant Blue KN-R using TiO_2/BC composite as heterogeneous photocatalyst and adsorbent. *Chemosphere* **2018**, *206*, 777–783, doi:10.1016/j.chemosphere.2018.05.073.
28. Li, Y.K.; Zhang, P.; Wan, D.Y.; Xue, C.; Zhao, J.T.; Shao, G.S. Direct evidence of 2D/1D heterojunction enhancement on photocatalytic activity through assembling MoS_2 nanosheets onto super-long TiO2 nanofibers. *Appl. Surf. Sci.* **2020**, *504*, 10, doi:10.1016/j.apsusc.2019.144361.
29. Pelaez, M.; Nolan, N.T.; Pillai, S.C.; Seery, M.K.; Falaras, P.; Kontos, A.G.; Dunlop, P.S.M.; Hamilton, J.W.J.; Byrne, J.A.; O'Shea, K.; et al. A review on the visible light active titanium dioxide photocatalysts for environmental applications. *Appl. Catal. B Environ.* **2012**, *125*, 331–349, doi:10.1016/j.apcatb.2012.05.036.
30. Liu, W.; Zhao, X.; Borthwick, A.G.L.; Wang, Y.Q.; Ni, J.R. Dual-Enhanced Photocatalytic Activity of Fe-Deposited Titanate Nanotubes Used for Simultaneous Removal of As(III) and As(V). *ACS Appl. Mater. Interfaces* **2015**, *7*, 19726–19735, doi:10.1021/acsami.5b05263.
31. Cai, Z.; Zhao, X.; Wang, T.; Liu, W.; Zhao, D. Reusable Platinum-Deposited Anatase/Hexa-Titanate Nanotubes: Roles of Reduced and Oxidized Platinum on Enhanced Solar-Light-Driven Photocatalytic Activity. *ACS Sustain. Chem. Eng.* **2017**, *5*, 547–555, doi:10.1021/acssuschemeng.6b01931.
32. Shankar, R.; Shim, W.J.; An, J.G.; Yim, U.H. A practical review on photooxidation of crude oil: Laboratory lamp setup and factors affecting it. *Water Res.* **2015**, *68*, 304–315, doi:10.1016/j.watres.2014.10.012.
33. Tian, J.; Zhao, Z.H.; Kumar, A.; Boughton, R.I.; Liu, H. Recent progress in design, synthesis, and applications of one-dimensional TiO_2 nanostructured surface heterostructures: a review. *Chem. Soc. Rev.* **2014**, *43*, 6920–6937, doi:10.1039/c4cs00180j.
34. Dahl, M.; Liu, Y.; Yin, Y. Composite Titanium Dioxide Nanomaterials. *Chem. Rev.* **2014**, *114*, 9853–9889, doi:10.1021/cr400634p
35. Hlekelele, L.; Durbach, S.H.; Chauke, V.P.; Dziike, F.; Franklyn, P.J. Resin-gel incorporation of high concentrations of W^{6+} and Zn^{2+} into TiO_2-anatase crystal to form quaternary mixed-metal oxides: effect on the a lattice parameter and photodegradation efficiency. *RSC Adv.* **2019**, *9*, 36875–36883, doi:10.1039/c9ra07355h.
36. Nzaba, S.K.M.; Nyoni, H.H.; Mamba, B.B.; Kuvarega, A.T. Comparative Study of Dendrimer-Templated Nitrogen-Platinum Co-Doped TiO_2 for the Photocatalytic Degradation of Azo Dyes in Contaminated Water. *Chemistryselect* **2019**, *4*, 12156–12163, doi:10.1002/slct.201903170.
37. Sun, D.W.; Li, Y.J.; Cao, T.P.; Zhao, Y.H.; Yang, D.K. Preparation of Dy^{3+}-doped YVO_4/TiO_2 Composite Nanofibers with Three-dimensional Net-like Structure and Enhanced Photocatalytic Activity for Hydrogen Evolution. *Chem. J. Chin. Univ. Chin.* **2019**, *40*, 2348–2353, doi:10.7503/cjcu20190302.

38. Deng, H.Y.; He, H.; Sun, S.J.; Zhu, X.T.; Zhou, D.X.; Han, F.X.; Huang, B.; Pan, X.J. Photocatalytic degradation of dye by Ag/TiO_2 nanoparticles prepared with different sol-gel crystallization in the presence of effluent organic matter. *Environ. Sci. Pollut. Res.* **2019**, *26*, 35900–35912, doi:10.1007/s11356-019-06728-0.
39. Yoshida, T.; Misu, Y.; Yamamoto, M.; Tanabe, T.; Kumagai, J.; Ogawa, S.; Yagi, S. Effects of the amount of Au nanoparticles on the visible light response of TiO_2 photocatalysts. Catal. Today 2020, 352, 34-38, doi:10.1016/j.cattod.2019.12.035.
40. Yang, L.X.; Chen, Z.; Zhang, J.; Wang, C.A. $SrTiO_3$/TiO_2 heterostructure nanowires with enhanced electron-hole separation for efficient photocatalytic activity. *Front. Mater. Sci.* **2019**, *13*, 342–351, doi:10.1007/s11706-019-0477-9.
41. Al Jitan, S.; Palmisano, G.; Garlisi, C. Synthesis and Surface Modification of TiO2-Based Photocatalysts for the Conversion of CO_2. *Catalysts* **2020**, *10*, 30, doi:10.3390/catal10020227.
42. Serpone, N. Is the band gap of pristine TiO_2 narrowed by anion- and cation-doping of titanium dioxide in second-generation photocatalysts? *J. Phys. Chem. B* **2006**, *110*, 24287–24293, doi:10.1021/jp065659r.
43. Devi, L.G.; Kavitha, R. A review on non metal ion doped titania for the photocatalytic degradation of organic pollutants under UV/solar light: Role of photogenerated charge carrier dynamics in enhancing the activity. *Appl. Catal. B-Environ.* **2013**, *140*, 559–587, doi:10.1016/j.apcatb.2013.04.035.
44. Asahi, R.; Morikawa, T.; Irie, H.; Ohwaki, T. Nitrogen-Doped Titanium Dioxide as Visible-Light-Sensitive Photocatalyst: Designs, Developments, and Prospects. *Chem. Rev.* **2014**, *114*, 9824–9852, doi:10.1021/cr5000738
45. Liao, F.; Chu, L.F.; Guo, C.X.; Guo, Y.J.; Ke, Q.F.; Guo, Y.P. Ytterbium Doped TiO_2 Nanofibers on Activated Carbon Fibers Enhances Adsorption and Photocatalytic Activities for Toluene Removal. *Chemistryselect* **2019**, *4*, 9222–9231.
46. Suarez, S.; Jansson, I.; Ohtani, B.; Sanchez, B. From titania nanoparticles to decahedral anatase particles: Photocatalytic activity of TiO_2/zeolite hybrids for VOCs oxidation. *Catal Today* **2019**, *326*, 2–7.
47. Liang, H.; Wang, Z.Q.; Liao, L.M.; Chen, L.; Li, Z.; Feng, J. High performance photocatalysts: Montmorillonite supported-nano TiO_2 composites. *Optik* **2017**, *136*, 44–51, doi:10.1016/j.ijleo.2017.02.018.
48. Zhu, P.F.; Ren, Z.H.; Wang, R.X.; Duan, M.; Xie, L.S.; Xu, J.; Tian, Y.J. Preparation and visible photocatalytic dye degradation of Mn-TiO_2/sepiolite photocatalysts. *Front. Mater. Sci.* **2020**, *14*, 33–42, doi:10.1007/s11706-020-0486-8.
49. Saqib, N.U.; Adnan, R.; Shah, I. Zeolite supported TiO_2 with enhanced degradation efficiency for organic dye under household compact fluorescent light. *Mater. Res. Express* **2019**, *6*, 13, doi:10.1088/2053-1591/ab2eb8.
50. Malakootian, M.; Nasiri, A.; Gharaghani, M.A. Photocatalytic degradation of ciprofloxacin antibiotic by TiO_2 nanoparticles immobilized on a glass plate. *Chem. Eng. Commun.* **2020**, *207*, 56–72, doi:10.1080/00986445.2019.1573168.
51. Espino-Estevez, M.R.; Fernandez-Rodriguez, C.; Gonzalez-Diaz, O.M.; Navio, J.A.; Fernandez-Hevia, D.; Dona-Rodriguez, J.M. Enhancement of stability and photoactivity of TiO_2 coatings on annular glass reactors to remove emerging pollutants from waters. *Chem. Eng. J.* **2015**, *279*, 488–497, doi:10.1016/j.cej.2015.05.038.
52. Pierpaoli, M.; Lewkowicz, A.; Rycewi'cz, M.; Szczodrowski, K.; Ruello, M.L.; Bogdanowicz, R. Enhanced photocatalytic activity of transparent carbon nanowall/TiO_2 heterostructures. *Mater. Lett.* **2020**, *262*.
53. Chu, Z.D.; Qiu, L.L.; Chen, Y.; Zhuang, Z.S.; Du, P.F.; Xiong, J. TiO_2-loaded carbon fiber: Microwave hydrothermal synthesis and photocatalytic activity under UV light irradiation. *J. Phys. Chem. Solids* **2020**, *136*, 7, doi:10.1016/j.jpcs.2019.109138.
54. Hu, C.Y.; Lei, E.; Hu, K.K.; Lai, L.Y.; Zhao, D.; Zhao, W.; Rong, H. Simple synthesis of 3D flower-like g-C_3N_4/TiO_2 composite microspheres for enhanced visible-light photocatalytic activity. *J. Mater. Sci.* **2020**, *55*, 151–162, doi:10.1007/s10853-019-03953-3.
55. Cunha, D.L.; Kuznetsov, A.; Araujo, J.R.; Neves, R.S.; Archanjo, B.S.; Canela, M.C.; Marques, M. Optimization of Benzodiazepine Drugs Removal from Water by Heterogeneous Photocatalysis Using TiO_2/Activated Carbon Composite. *Water Air Soil Pollut.* **2019**, *230*, 17, doi:10.1007/s11270-019-4202-1.
56. Zhang, Y.Y.; Jiang, Z.L.; Huang, J.Y.; Lim, L.Y.; Li, W.L.; Deng, J.Y.; Gong, D.G.; Tang, Y.X.; Lai, Y.K.; Chen, Z. Titanate and titania nanostructured materials for environmental and energy applications: a review. *RSC Adv.* **2015**, *5*, 79479–79510, doi:10.1039/c5ra11298b.

57. Zhao, X.; Cai, Z.Q.; Wang, T.; O'Reilly, S.E.; Liu, W.; Zhao, D.Y. A new type of cobalt-deposited titanate nanotubes for enhanced photocatalytic degradation of phenanthrene. *Appl. Catal. B Environ.* **2016**, *187*, 134–143, doi:10.1016/j.apcatb.2016.01.010.
58. Doong, R.-a.; Liao, C.-Y. Enhanced visible-light-responsive photodegradation of bisphenol A by Cu, N-codoped titanate nanotubes prepared by microwave-assisted hydrothermal method. *J. Hazard. Mater.* **2017**, *322*, 254–262, doi:doi:10.1016/j.jhazmat.2016.02.065.
59. Liu, W.; Sun, W.L.; Borthwick, A.G.L.; Wang, T.; Li, F.; Guan, Y.D. Simultaneous removal of Cr(VI) and 4-chlorophenol through photocatalysis by a novel anatase/titanate nanosheet composite: Synergetic promotion effect and autosynchronous doping. *J. Hazard. Mater.* **2016**, *317*, 385–393, doi:10.1016/j.jhazmat.2016.06.002.
60. Zhao, X.; Du, P.H.; Cai, Z.Q.; Wang, T.; Fu, J.; Liu, W. Photocatalysis of bisphenol A by an easy-settling titania/titanate composite: Effects of water chemistry factors, degradation pathway and theoretical calculation. *Environ. Pollut.* **2018**, *232*, 580–590, doi:10.1016/j.envpol.2017.09.094.
61. Li, F.; Du, P.H.; Liu, W.; Li, X.S.; Ji, H.D.; Duan, J.; Zhao, D.Y. Hydrothermal synthesis of graphene grafted titania/titanate nanosheets for photocatalytic degradation of 4-chlorophenol: Solar-light-driven photocatalytic activity and computational chemistry analysis. *Chem. Eng. J.* **2018**, *331*, 685–694, doi:10.1016/j.cej.2017.09.036.
62. Cheng, K.Y.; Cai, Z.Q.; Fu, J.; Sun, X.B.; Sun, W.L.; Chen, L.; Zhang, D.D.; Liu, W. Synergistic adsorption of Cu(II) and photocatalytic degradation of phenanthrene by a jaboticaba-like TiO_2/titanate nanotube composite: An experimental and theoretical study. *Chem. Eng. J.* **2019**, *358*, 1155–1165, doi:10.1016/j.cej.2018.10.114.
63. Ji, H.D.; Du, P.H.; Zhao, D.Y.; Li, S.; Sun, F.B.; Duin, E.C.; Liu, W. 2D/1D graphitic carbon nitride/titanate nanotubes heterostructure for efficient photocatalysis of sulfamethazine under solar light: Catalytic "hot spots" at the rutile-anatase-titanate interfaces. *Appl. Catal. B* **2020**, *263*, 12, doi:10.1016/j.apcatb.2019.118357.
64. Tu, H.; Li, D.; Yi, Y.; Liu, R.; Wu, Y.; Dong, X.Y.; Shi, X.W.; Deng, H.B. Incorporation of rectorite into porous polycaprolactone/TiO_2 nanofibrous mats for enhancing photocatalysis properties towards organic dye pollution. *Compos. Commun.* **2019**, *15*, 58–63, doi:10.1016/j.coco.2019.06.006.
65. Ni, Y.H.; Yan, K.; Xu, F.Y.; Zhong, W.B.; Zhao, Q.H.; Liu, K.; Yan, K.L.; Wang, D. Synergistic effect on TiO_2 doped poly (vinyl alcohol-co-ethylene) nanofibrous film for filtration and photocatalytic degradation of methylene blue. *Compos. Commun.* **2019**, *12*, 112–116, doi:10.1016/j.coco.2019.01.007.
66. Mohsenzadeh, M.; Mirbagheri, S.A.; Sabbaghi, S. Photocatalytic degradation of 1,2-dichloroethane using immobilized PANI-TiO_2 nanocomposite in a pilot-scale packed bed reactor. *Desalin. Water Treat.* **2019**, *155*, 72–83, doi:10.5004/dwt.2019.23875.
67. Qin, Y.Y.; Li, H.; Lu, J.; Meng, F.Y.; Ma, C.C.; Yan, Y.S.; Meng, M.J. Nitrogen-doped hydrogenated TiO_2 modified with CdS nanorods with enhanced optical absorption, charge separation and photocatalytic hydrogen evolution. *Chem. Eng. J.* **2020**, *384*.
68. Ratova, M.; West, G.T.; Kelly, P.J.; Xia, X.; Gao, Y. Synergistic effect of doping with nitrogen and molybdenum on the photocatalytic properties of thin titania films. *Vacuum* **2015**, *114*, 205–212.
69. Kovalevskiy, N.; Selishchev, D.; Svintsitskiy, D.; Selishcheva, S.; Berezin, A.; Kozlov, D. Synergistic effect of polychromatic radiation on visible light activity of N-doped TiO_2 photocatalyst. *Catal. Commun.* **2020**, *134*.
70. Fang, W.Z.; Xing, M.Y.; Zhang, J.L. Modifications on reduced titanium dioxide photocatalysts: A review. *J. Photochem. Photobio. C* **2017**, *32*, 21–39.
71. Reda, S.M.; Khairy, M.; Mousa, M.A. Photocatalytic activity of nitrogen and copper doped TiO_2 nanoparticles prepared by microwave-assisted sol-gel process. *Arab. J. Chem.* **2020**, *13*, 86–95.
72. Jin, X.D.; Zhou, X.Q.; Sun, P.; Lin, S.Y.; Cao, W.B.; Li, Z.F.; Liu, W.X. Photocatalytic degradation of norfloxacin using N-doped TiO_2: Optimization, mechanism, identification of intermediates and toxicity evaluation. *Chemosphere* **2019**, *237*.
73. Ji, L.J.; Zhou, S.; Liu, X.; Gong, M.D.; Xu, T. Synthesis of carbon- and nitrogen-doped TiO_2/carbon composite fibers by a surface-hydrolyzed PAN fiber and their photocatalytic property. *J. Mater. Sci.* **2020**, *55*, 2471–2481.
74. Asahi, R.; Morikawa, T.; Ohwaki, T.; Aoki, K.; Taga, Y. Visible-light photocatalysis in nitrogen-doped titanium oxides. *Science* **2001**, *293*, 269–271, doi:10.1126/science.1061051.

75. Li, H.; Hao, Y.B.; Lu, H.Q.; Liang, L.P.; Wang, Y.Y.; Qiu, J.H.; Shi, X.C.; Wang, Y.; Yao, J.F. systematic study on visible-light N-doped TiO_2 photocatalyst obtained from ethylenediamine by sol-gel method. *Appl. Surf. Sci.* **2015**, *344*, 112–118, doi:10.1016/j.apsusc.2015.03.071.
76. Jyothi, M.S.; Laveena, P.D.; Shwetharani, R.; Balakrishna, G.R. Novel hydrothermal method for effective doping of N and F into nano Titania for both, energy and environmental applications. *Mater. Res. Bull.* **2016**, *74*, 478–484, doi:10.1016/j.materresbull.2015.11.020.
77. Rahbar, M.; Mehrzad, M.; Behpour, M.; Mohammadi-Aghdam, S.; Ashrafi, M. S, N co-doped carbon quantum dots/TiO_2 nanocomposite as highly efficient visible light photocatalyst. *Nanotechnology* **2019**, *30*, 16, doi:10.1088/1361-6528/ab40dc.
78. Liu, D.; Wang, J.Q.; Zhou, J.; Xi, Q.H.; Li, X.; Nie, E.; Piao, X.Q.; Sun, Z. Fabricating I doped TiO_2 photoelectrode for the degradation of diclofenac: Performance and mechanism study. *Chem. Eng. J.* **2019**, *369*, 968–978, doi:10.1016/j.cej.2019.03.140.
79. Ichihara, F.; Sieland, F.; Pang, H.; Philo, D.; Duong, A.T.; Chang, K.; Kako, T.; Bahnemann, D.W.; Ye, J.H. Photogenerated Charge Carriers Dynamics on La- and/or Cr-Doped $SrTiO_3$ Nanoparticles Studied by Transient Absorption Spectroscopy. *J. Phys. Chem. C* **2020**, *124*, 1292–1302, doi:10.1021/acs.jpcc.9b09324.
80. Tian, L.J.; Xing, L.; Shen, X.L.; Li, Q.H.; Ge, S.J.; Liu, B.K.; Jie, L. Visible light enhanced Fe-I-TiO_2 photocatalysts for the degradation of gaseous benzene. *Atmos. Pollut. Res.* **2020**, *11*, 179–185, doi:10.1016/j.apr.2019.10.005.
81. Razali, M.H.; Noor, A.F.M.; Yusoff, M. Physicochemical Properties of a Highly Efficient Cu-Ion-Doped TiO_2 Nanotube Photocatalyst for the Degradation of Methyl Orange Under Sunlight. *J. Nanosci. Nanotechnol.* **2020**, *20*, 965–972.
82. Li, Z.; Tian, B.; Zhen, W.L.; Wu, Y.Q.; Lu, G.X. Inhibition of hydrogen and oxygen recombination using oxygen transfer reagent hemin chloride in Pt/TiO_2 dispersion for photocatalytic hydrogen generation. *Appl. Catal. B* **2017**, *203*, 408–415, doi:10.1016/j.apcatb.2016.10.049.
83. Yu, Y.Q.; Zhu, X.R.; Wang, L.R.; Wu, F.S.; Liu, S.L.; Chang, C.Y.; Luo, X.G. A simple strategy to design 3-layered Au-TiO_2 dual nanoparticles immobilized cellulose membranes with enhanced photocatalytic activity. *Carbohydr. Polym.* **2020**, *231*.
84. Surya, C.; John, N.A.A.; Pandiyan, V.; Ravikumar, S.; Amutha, P.; Sobral, A.J.F.N.; Krishnakumar, B. Costus speciosus leaf extract assisted CS-Pt-TiO_2 composites: Synthesis, characterization and their bio and photocatalytic applications. *J. Mol. Struct.* **2019**, *1195*, 787–795.
85. Maarisetty, D.; Baral, S.S. Defect-induced enhanced dissociative adsorption, optoelectronic properties and interfacial contact in Ce doped TiO_2: Solar photocatalytic degradation of Rhodamine B. *Ceram Int.* **2019**, *45*, 22253–22263.
86. Zhao, J.; Chen, X.Y.; Zhou, Y.H.; Tian, H.J.; Guo, Q.J.; Hu, X.D. Efficient removal of oil pollutant via simultaneous adsorption and photocatalysis using La-N-TiO_2-cellulose/SiO_2 difunctional aerogel composite. *Res. Chem. Intermediat* **2020**.
87. Liang, J.C.; Wang, J.Y.; Song, K.X.; Wang, X.F.; Yu, K.F.; Liang, C. Enhanced photocatalytic activities of Nd-doped TiO_2 under visible light using a facile sol-gel method. *J. Rare Earth* **2020**, *38*, 148–156.
88. Hu, Z.; Yang, C.; Lv, K.; Li, X.; Li, Q.; Fan, J. Single atomic Au induced dramatic promotion of the photocatalytic activity of TiO_2 hollow microspheres. *Chem. Commun. Camb. Engl.* **2020**, doi: 10.1039/c9cc08578e, doi:10.1039/c9cc08578e.
89. Hayashi, T.; Nakamura, K.; Suzuki, T.; Saito, N.; Murakami, Y. OH radical formation by the photocatalytic reduction reactions of H_2O_2 on the surface of plasmonic excited Au-TiO2 photocatalysts. *Chem. Phys. Lett.* **2020**, *739*, 136958.
90. Jeantelot, G.; Qureshi, M.; Harb, M.; Ould-Chikh, S.; Anjum, D.H.; Abou-Hamad, E.; Aguilar-Tapia, A.; Hazemann, J.L.; Takanabe, K.; Basset, J.M. TiO_2-supported Pt single atoms by surface organometallic chemistry for photocatalytic hydrogen evolution. *Phys. Chem. Chem. Phys.* **2019**, *21*, 24429–24440.
91. Singhal, N.; Kumar, U. Noble metal modified TiO_2: selective photoreduction of CO_2 to hydrocarbons. *Mol. Catal.* **2017**, *439*, 91–99.
92. Gao, P.; Yang, L.B.; Xiao, S.T.; Wang, L.Y.; Guo, W.; Lu, J.H. Effect of Ru, Rh, Mo, and Pd Adsorption on the Electronic and Optical Properties of Anatase TiO_2(101): A DFT Investigation. *Materials* **2019**, *12*.
93. Liu, Y.; Xiao, Z.Z.; Cao, S.; Li, J.H.; Piao, L.Y. Controllable synthesis of Au-TiO_2 nanodumbbell photocatalysts with spatial redox region. *Chinese J. Catal.* **2020**, *41*, 219–226.

94. Khatun, F.; Abd Aziz, A.; Sim, L.C.; Monir, M.U. Plasmonic enhanced Au decorated TiO2 nanotube arrays as a visible light active catalyst towards photocatalytic CO_2 conversion to CH_4. *J. Environ. Chem. Eng.* **2019**, *7*.
95. Sacco, O.; Murcia, J.J.; Lara, A.E.; Hernandez-Laverde, M.; Rojas, H.; Navio, J.A.; Hidalgo, M.C.; Vaiano, V. Pt-TiO_2-Nb_2O_5 heterojunction as effective photocatalyst for the degradation of diclofenac and ketoprofen. *Mat. Sci. Semicon Proc.* **2020**, *107*, 13, doi:10.1016/j.mssp.2019.104839.
96. Qu, J.F.; Chen, D.Y.; Li, N.J.; Xu, Q.F.; Li, H.; He, J.H.; Lu, J.M. Ternary photocatalyst of atomic-scale Pt coupled with MoS_2 co-loaded on TiO_2 surface for highly efficient degradation of gaseous toluene. *Appl. Catal. B* **2019**, *256*.
97. Ouyang, W.Y.; Munoz-Batista, M.J.; Kubacka, A.; Luque, R.; Fernandez-Garcia, M. Enhancing photocatalytic performance of TiO_2 in H_2 evolution via Ru co-catalyst deposition. *Appl. Catal B Environ.* **2018**, *238*, 434–443.
98. Li, F.; Huang, H.B.; Li, G.S.; Leung, D.Y.C. TiO_2 nanotube arrays modified with nanoparticles of platinum group metals (Pt, Pd, Ru): enhancement on photoelectrochemical performance. *J. Nanopart Res.* **2019**, *21*.
99. Sato, S.; White, J.M. Photodecomposition of water over Pt/TiO_2 catalysts. *Chem. Phys. Lett.* **1980**, *72*, 83–86.
100. Kennedy, J.C.; Datye, A.K. Photothermal heterogeneous oxidation of ethanol over Pt/TiO_2. *J. Catal.* **1998**, *179*, 375–389, doi:10.1006/jcat.1998.2242.
101. Ji, L.J.; Qin, X.; Zheng, J.J.; Zhou, S.; Xu, T.; Shi, G.J. Synthesis of Ag-Carbon-TiO_2 composite tubes and their antibacterial and organic degradation properties. *J. Sol Gel Sci. Technol.* **2020**, *93*, 291–301, doi:10.1007/s10971-019-05197-8.
102. Shan, R.; Lu, L.L.; Gu, J.; Zhang, Y.Y.; Yuan, H.R.; Chen, Y.; Luo, B. Photocatalytic degradation of methyl orange by Ag/TiO2/biochar composite catalysts in aqueous solutions. *Mater. Sci. Semicond. Process.* **2020**, *114*, 12, doi:10.1016/j.mssp.2020.105088.
103. Jaafar, F.; Jalil, A.A.; Triwahyono, S.; Efendi, J.; Mukti, R.R.; Jusoh, R.; Jusoh, N.W.C.; Karim, A.H.; Salleh, N.F.M.; Suendo, V. Direct in situ activation of Ag^0 nanoparticles in synthesis of Ag/TiO_2 and its photoactivity. *Appl. Surf. Sci.* **2015**, *338*, 75–84, doi:10.1016/j.apsusc.2015.02.106.
104. Zhu, D.H.; Long, L.; Sun, J.Y.; Wan, H.Q.; Zheng, S.R. Highly active and selective catalytic hydrogenation of p-chloronitrobenzene to p-chloroaniline on Pt@Cu/TiO_2. *Appl. Surf. Sci.* **2020**, *504*.
105. Nyankson, E.; Agyei-Tuffour, B.; Adjasoo, J.; Ebenezer, A.; Dodoo-Arhin, D.; Yaya, A.; Mensah, B.; Efavi, J.K. Synthesis and Application of Fe-Doped TiO_2-Halloysite Nanotubes Composite and Their Potential Application in Water Treatment. *Adv. Mater. Sci. Eng.* **2019**, *2019*.
106. Komaraiah, D.; Radha, E.; Sivakumar, J.; Reddy, M.V.R.; Sayanna, R. Structural, optical properties and photocatalytic activity of Fe^{3+} doped TiO_2 thin films deposited by sol-gel spin coating. *Surf. Interfaces* **2019**, *17*.
107. Bhardwaj, S.; Dogra, D.; Pal, B.; Singh, S. Photodeposition time dependant growth, size and photoactivity of Ag and Cu deposited TiO_2 nanocatalyst under solar irradiation. *Sol. Energy* **2019**, *194*, 618–627.
108. Ghanbari, S.; Givianrad, M.H.; Azar, P.A. Synthesis and characterization of visible light driven N-Fe-codoped TiO_2/SiO_2 for simultaneous photoremoval of Cr (VI) and azo dyes in a novel fixed bed continuous flow photoreactor. *Can. J. Chem. Eng.* **2020**, *98*, 705–716, doi:10.1002/cjce.23660.
109. Ahadi, S.; Moalej, N.S.; Sheibani, S. Characteristics and photocatalytic behavior of Fe and Cu doped TiO_2 prepared by combined sol-gel and mechanical alloying. *Solid State Sci.* **2019**, *96*.
110. Zhang, J.H.; Fu, D.; Wang, S.Q.; Hao, R.L.; Xie, Y.X. Photocatalytic removal of chromium(VI) and sulfite using transition metal (Cu, Fe, Zn) doped TiO_2 driven by visible light: Feasibility, mechanism and kinetics. *J. Ind. Eng. Chem.* **2019**, *80*, 23–32.
111. Khan, M.A.M.; Siwach, R.; Kumar, S.; Alhazaa, A.N. Role of Fe doping in tuning photocatalytic and photoelectrochemical properties of TiO_2 for photodegradation of methylene blue. *Opt. Laser Technol.* **2019**, *118*, 170–178.
112. Bhatia, V.; Dhir, A. Transition metal doped TiO_2 mediated photocatalytic degradation of anti-inflammatory drug under solar irradiations. *J. Environ. Chem. Eng.* **2016**, *4*, 1267–1273.
113. Stucchi, M.; Boffito, D.C.; Pargoletti, E.; Cerrato, G.; Bianchi, C.L.; Cappelletti, G. Nano-MnO_2 Decoration of TiO_2 Microparticles to Promote Gaseous Ethanol Visible Photoremoval. *Nanomaterials* **2018**, *8*, 12, doi:10.3390/nano8090686.

114. Choi, W.; Termin, A.; Hoffmann, M.R. The Role of Metal Ion Dopants in Quantum-Sized TiO_2: Correlation between Photoreactivity and Charge Carrier Recombination Dynamics. *J. Phys. Chem.* **1994**, *98*, 13669–13679, doi:10.1021/j100102a038.
115. Du, X.-q.; Ma, X.-l.; Wang, Y.-j.; Gu, F.-n.; Zhang, J. Optimization of the Ge/TiO_2 catalyst for the degradation of ciprofloxacin by the response surface methodology. *Zhongguo Kangshengsu Zazhi* **2019**, *44*, 750–757.
116. Crisan, M.; Mardare, D.; Ianculescu, A.; Dragan, N.; Nitoi, I.; Crisan, D.; Voicescu, M.; Todan, L.; Oancea, P.; Adomnitei, C.; et al. Iron doped TiO_2 films and their photoactivity in nitrobenzene removal from water. *Appl. Surf. Sci.* **2018**, *455*, 201–215, doi:10.1016/j.apsusc.2018.05.124.
117. Gnanasekaran, L.; Hemamalini, R.; Saravanan, R.; Ravichandran, K.; Gracia, F.; Gupta, V.K. Intermediate state created by dopant ions (Mn, Co and Zr) into TiO_2 nanoparticles for degradation of dyes under visible light. *J. Mol. Liq.* **2016**, *223*, 652–659, doi:10.1016/j.molliq.2016.08.105.
118. Huang, J.G.; Guo, X.T.; Wang, B.; Li, L.Y.; Zhao, M.X.; Dong, L.L.; Liu, X.J.; Huang, Y.T. Synthesis and Photocatalytic Activity of Mo-Doped TiO_2 Nanoparticles. *J. Spectrosc.* **2015**, 1–8, doi:10.1155/2015/681850.
119. Wang, Q.; Jin, R.; Zhang, M.; Gao, S. Solvothermal preparation of Fe-doped TiO_2 nanotube arrays for enhancement in visible light induced photoelectrochemical performance. *J. Alloys Compd*. **2017**, *690*, 139–144.
120. Vinodgopal, K.; Kamat, P.V. Enhanced Rates of Photocatalytic Degradation of an Azo Dye Using SnO_2/TiO_2 Coupled Semiconductor Thin Films. *Environ. Sci. Technol.* **1995**, *29*, 841–845, doi:10.1021/es00003a037.
121. Low, J.; Yu, J.; Jaroniec, M.; Wageh, S.; Al-Ghamdi, A.A. Heterojunction Photocatalysts. *Adv. Mater.* **2017**, *29*, 1601694, doi:10.1002/adma.201601694.
122. Kaur, P.K.; Badru, R.; Singh, P.P.; Kaushal, S. Photodegradation of organic pollutants using heterojunctions: A review. *J. Environ. Chem. Eng.* **2020**, *8*, 20, doi:10.1016/j.jece.2020.103666.
123. Li, H.J.; Zhou, Y.; Tu, W.G.; Ye, J.H.; Zou, Z.G. State-of-the-Art Progress in Diverse Heterostructured Photocatalysts toward Promoting Photocatalytic Performance. *Adv. Funct. Mater.* **2015**, *25*, 998–1013, doi:10.1002/adfm.201401636.
124. Dursun, S.; Kaya, I.C.; Kalem, V.; Akyildiz, H. UV/visible light active $CuCrO_2$ nanoparticle-SnO_2 nanofiber p-n heterostructured photocatalysts for photocatalytic applications. *Dalton Trans.* **2018**, *47*, 14662–14678, doi:10.1039/c8dt02850h.
125. Zhang, W.P.; Xiao, X.Y.; Li, Y.; Zeng, X.Y.; Zheng, L.L.; Wan, C.X. Liquid-exfoliation of layered MoS_2 for enhancing photocatalytic activity of TiO_2/g-C_3N_4 photocatalyst and DFT study. *Appl. Surf. Sci.* **2016**, *389*, 496–506, doi:10.1016/j.apsusc.2016.07.154.
126. Yang, L.; Gao, M.G.; Dai, B.; Guo, X.H.; Liu, Z.Y.; Peng, B.H. Synthesis of spindle-shaped AgI/TiO_2 nanoparticles with enhanced photocatalytic performance. *Appl. Surf. Sci.* **2016**, *386*, 337–344, doi:10.1016/j.apsusc.2016.06.043.
127. Demirci, S.; Dikici, T.; Yurddaskal, M.; Gultekin, S.; Toparli, M.; Celik, E. Synthesis and characterization of Ag doped TiO_2 heterojunction films and their photocatalytic performances. *Appl. Surf. Sci.* **2016**, *390*, 591–601, doi:10.1016/j.apsusc.2016.08.145.
128. Sarkar, A.; Gracia-Espino, E.; Wagberg, T.; Shchukarev, A.; Mohl, M.; Rautio, A.R.; Pitkanen, O.; Sharifi, T.; Kordas, K.; Mikkola, J.P. Photocatalytic reduction of CO_2 with H_2O over modified TiO_2 nanofibers: Understanding the reduction pathway. *Nano Res.* **2016**, *9*, 1956–1968, doi:10.1007/s12274-016-1087-9.
129. Low, J.X.; Cheng, B.; Yu, J.G. Surface modification and enhanced photocatalytic CO2 reduction performance of TiO_2: a review. *Appl. Surf. Sci.* **2017**, *392*, 658–686, doi:10.1016/j.apsusc.2016.09.093.
130. Moniz, S.J.A.; Shevlin, S.A.; Martin, D.J.; Guo, Z.X.; Tang, J.W. Visible-light driven heterojunction photocatalysts for water splitting—a critical review. *Energy Environ. Sci.* **2015**, *8*, 731–759, doi:10.1039/c4ee03271c.
131. Kumar, A.; Khan, M.; He, J.H.; Lo, I.M.C. Recent developments and challenges in practical application of visible-light-driven TiO_2-based heterojunctions for PPCP degradation: A critical review. *Water Res.* **2020**, *170*, 18, doi:10.1016/j.watres.2019.115356.
132. Ong, W.J.; Tan, L.L.; Ng, Y.H.; Yong, S.T.; Chai, S.P. Graphitic Carbon Nitride (g-C_3N_4)-Based Photocatalysts for Artificial Photosynthesis and Environmental Remediation: Are We a Step Closer To Achieving Sustainability? *Chem. Rev.* **2016**, *116*, 7159–7329, doi:10.1021/acs.chemrev.6b00075.
133. Ahmed, S.N.; Haider, W. Heterogeneous photocatalysis and its potential applications in water and wastewater treatment: a review. *Nanotechnology* **2018**, *29*, 30, doi:10.1088/1361-6528/aac6ea.

134. McDaniel, H.; Heil, P.E.; Tsai, C.L.; Kim, K.; Shim, M. Integration of Type II Nanorod Heterostructures into Photovoltaics. *ACS Nano* **2011**, *5*, 7677–7683, doi:10.1021/nn2029988.
135. Gou, J.F.; Ma, Q.L.; Deng, X.Y.; Cui, Y.Q.; Zhang, H.X.; Cheng, X.W.; Li, X.L.; Xie, M.Z.; Cheng, Q.F. Fabrication of Ag_2O/TiO_2-Zeolite composite and its enhanced solar light photocatalytic performance and mechanism for degradation of norfloxacin. *Chem. Eng. J.* **2017**, *308*, 818–826, doi:10.1016/j.cej.2016.09.089.
136. Wang, W.; Fang, J.J.; Shao, S.F.; Lai, M.; Lu, C.H. Compact and uniform TiO_2@g-C_3N_4 core-shell quantum heterojunction for photocatalytic degradation of tetracycline antibiotics. *Appl. Catal. B* **2017**, *217*, 57–64, doi:10.1016/j.apcatb.2017.05.037.
137. Hou, H.J.; Zhang, X.H.; Huang, D.K.; Ding, X.; Wang, S.Y.; Yang, X.L.; Li, S.Q.; Xiang, Y.G.; Chen, H. Conjugated microporous poly(benzothiadiazole)/TiO2 heterojunction for visible-light-driven H_2 production and pollutant removal. *Appl. Catal. B* **2017**, *203*, 563–571, doi:10.1016/j.apcatb.2016.10.059.
138. Ganguly, P.; Mathew, S.; Clarizia, L.; Kumar, R.S.; Akande, A.; Hinder, S.; Breen, A.; Pillai, S.C. Theoretical and experimental investigation of visible light responsive $AgBiS_2$-TiO_2 heterojunctions for enhanced photocatalytic applications. *Appl. Catal. B* **2019**, *253*, 401–418, doi:10.1016/j.apcatb.2019.04.033.
139. Liu, Z.; Tian, J.; Zeng, D.B.; Yu, C.L.; Huang, W.Y.; Yang, K.; Liu, X.Q.; Liu, H. Binary-phase TiO_2 modified Bi_2MoO_6 crystal for effective removal of antibiotics under visible light illumination. *Mater. Res. Bull.* **2019**, *112*, 336–345, doi:10.1016/j.materresbull.2019.01.002.
140. Yu, J.G.; Wang, S.H.; Low, J.X.; Xiao, W. Enhanced photocatalytic performance of direct Z-scheme g-C_3N_4-TiO_2 photocatalysts for the decomposition of formaldehyde in air. *Phys. Chem. Chem. Phys.* **2013**, *15*, 16883–16890, doi:10.1039/c3cp53131g.
141. Mei, Q.F.; Zhang, F.Y.; Wang, N.; Lu, W.S.; Su, X.T.; Wang, W.; Wu, R.L. Photocatalysts: Z-Scheme Heterojunction Constructed with Titanium Dioxide. *Chin. J. Inorg. Chem.* **2019**, *35*, 1321–1339, doi:10.11862/cjic.2019.167.
142. Li, H.J.; Tu, W.G.; Zhou, Y.; Zou, Z.G. Z-Scheme Photocatalytic Systems for Promoting Photocatalytic Performance: Recent Progress and Future Challenges. *Adv. Sci.* **2016**, *3*, 12, doi:10.1002/advs.201500389.
143. Qi, K.Z.; Cheng, B.; Yu, J.G.; Ho, W.K. A review on TiO_2-based Z-scheme photocatalysts. *Chin. J. Catal.* **2017**, *38*, 1936–1955, doi:10.1016/s1872-2067(17)62962-0.
144. Low, J.X.; Jiang, C.; Cheng, B.; Wageh, S.; Al-Ghamdi, A.A.; Yu, J.G. A Review of Direct Z-Scheme Photocatalysts. *Small Methods* **2017**, *1*, 21, doi:10.1002/smtd.201700080.
145. Meng, S.G.; Zhang, J.F.; Chen, S.F.; Zhang, S.J.; Huang, W.X. Perspective on construction of heterojunction photocatalysts and the complete utilization of photogenerated charge carriers. *Appl. Surf. Sci.* **2019**, *476*, 982–992, doi:10.1016/j.apsusc.2019.01.246.
146. Wang, F.L.; Wu, Y.L.; Wang, Y.F.; Li, J.H.; Jin, X.Y.; Zhang, Q.X.; Li, R.B.; Yan, S.C.; Liu, H.J.; Feng, Y.P.; et al. Construction of novel Z-scheme nitrogen-doped carbon dots/{001} TiO_2 nanosheet photocatalysts for broad-spectrum-driven diclofenac degradation: Mechanism insight, products and effects of natural water matrices. *Chem. Eng. J.* **2019**, *356*, 857–868, doi:10.1016/j.cej.2018.09.092.
147. Hao, J.G.; Zhang, S.F.; Ren, F.; Wang, Z.W.; Lei, J.F.; Wang, X.N.; Cheng, T.; Li, L.B. Synthesis of TiO_2@g-C_3N_4 core-shell nanorod arrays with Z-scheme enhanced photocatalytic activity under visible light. *J. Colloid Interface Sci.* **2017**, *508*, 419–425, doi:10.1016/j.jcis.2017.08.065.
148. Liao, W.J.; Murugananthan, M.; Zhang, Y.R. Synthesis of Z-scheme g-C_3N_4-Ti^{3+}/TiO_2 material: an efficient visible light photoelectrocatalyst for degradation of phenol. *Phys. Chem. Chem. Phys.* **2015**, *17*, 8877–8884, doi:10.1039/c5cp00639b.
149. Shayegan, Z.; Lee, C.S.; Haghighat, F. TiO_2 photocatalyst for removal of volatile organic compounds in gas phase - A review. *Chem. Eng. J.* **2018**, *334*, 2408–2439, doi:10.1016/j.cej.2017.09.153.
150. Basavarajappa, P.S.; Patil, S.B.; Ganganagappa, N.; Reddy, K.R.; Raghu, A.V.; Reddy, C.V. Recent progress in metal-doped TiO_2, non-metal doped/codoped TiO_2 and TiO_2 nanostructured hybrids for enhanced photocatalysis. *Int. J. Hydrog. Energy* **2020**, *45*, 7764–7778, doi:10.1016/j.ijhydene.2019.07.241.
151. Li, S.Y.; Yang, Y.L.; Su, Q.; Liu, X.Y.; Zhao, H.P.; Zhao, Z.X.; Li, J.; Jin, C. Synthesis and photocatalytic activity of transition metal and rare earth element co-doped TiO_2 nano particles. *Mater. Lett.* **2019**, *252*, 123–125, doi:10.1016/j.matlet.2019.05.123.
152. Oladipo, G.O.; Akinlabi, A.K.; Alayande, S.O.; Msagati, T.A.M.; Nyoni, H.H.; Ogunyinka, O.O. Synthesis, characterization, and photocatalytic activity of silver and zinc co-doped TiO_2 nanoparticle for photodegradation of methyl orange dye in aqueous solution. *Can. J. Chem.* **2019**, *97*, 642–650, doi:10.1139/cjc-2018-0308.

153. Shahan, M.; Ahmed, A.M.; Shehata, N.; Betiha, M.A.; Rabie, A.M. Ni-doped and Ni/Cr co-doped TiO_2 nanotubes for enhancement of photocatalytic degradation of methylene blue. *J. Colloid Interface Sci.* **2019**, *555*, 31–41, doi:10.1016/j.jcis.2019.07.070.
154. Xia, H.Y.; Liu, G.Y.; Zhang, R.; Song, L.F.; Chen, H.X. The Photocatalytic Degradation of Vehicle Exhausts by an Fe/N/Co-TiO_2 Waterborne Coating under Visible Light. *Materials* **2019**, *12*, 17, doi:10.3390/ma12203378.
155. Sun, M.X.; Yao, Y.; Ding, W.; Anandan, S. N/Ti^{3+} co-doping biphasic TiO2/Bi2WO6 heterojunctions: Hydrothermal fabrication and sonophotocatalytic degradation of organic pollutants. *J. Alloy. Compd.* **2020**, *820*, 9, doi:10.1016/j.jallcom.2019.153172.
156. Bayan, E.M.; Lupeiko, T.G.; Pustovaya, L.E.; Volkova, M.G.; Butova, V.V.; Guda, A.A. Zn-F co-doped TiO_2 nanomaterials: Synthesis, structure and photocatalytic activity. *J. Alloy. Compd.* **2020**, *822*, 10, doi:10.1016/j.jallcom.2020.153662.
157. Zhao, L.; Xie, Y.Z.; Lin, Q.Y.; Zheng, R.Z.; Diao, Y. Preparation of C, N and P co-doped TiO_2 and its photocatalytic activity under visible light. *Funct. Mater. Lett.* **2019**, *12*, 5, doi:10.1142/s1793604719500450.
158. Wang, H.X.; Zhu, L.N.; Guo, F.Q. Photoelectrocatalytic degradation of atrazine by boron-fluorine co-doped TiO_2 nanotube arrays. *Environ. Sci. Pollut. Res.* **2019**, *26*, 33847–33855, doi:10.1007/s11356-018-2569-y.
159. Yan, J.C.; Zhao, J.; Hao, L.; Hu, Y.F.; Liu, T.Y.; Guan, S.J.; Zhao, Q.; Zhu, Z.; Lu, Y. Low-temperature S-doping on N-doped TiO_2 films and remarkable enhancement on visible-light performance. *Mater. Res. Bull.* **2019**, *120*, 7, doi:10.1016/j.materresbull.2019.110594.
160. Mohamed, R.M.; Bahnemann, D.W.; Basaleh, A.S.; Qadah, R.H. Photo-catalytic destruction of acetaldehyde using cobalt, copper co-doped titania dioxide nanoparticles beneath Visible light. *Appl. Nanosci.* **2020**, *10*, 931–939, doi:10.1007/s13204-019-01157-4.
161. Pham, T.D.; Lee, B.K. Selective removal of polar VOCs by novel photocatalytic activity of metals co-doped TiO_2/PU under visible light. *Chem. Eng. J.* **2017**, *307*, 63–73, doi:10.1016/j.cej.2016.08.068.
162. Isari, A.A.; Hayati, F.; Kakavandi, B.; Rostami, M.; Motevassel, M.; Dehghanifard, E. N, Cu co-doped TiO_2@functionalized SWCNT photocatalyst coupled with ultrasound and visible-light: An effective sono-photocatalysis process for pharmaceutical wastewaters treatment. *Chem. Eng. J.* **2020**, *392*, 16, doi:10.1016/j.cej.2019.123685.
163. Sharotri, N.; Sharma, D.; Sud, D. Experimental and theoretical investigations of Mn-N-co-doped TiO_2 photocatalyst for visible light induced degradation of organic pollutants. *J. Mater. Res. Technol.* **2019**, *8*, 3995–4009, doi:10.1016/j.jmrt.2019.07.008.
164. Sirivallop, A.; Areerob, T.; Chiarakorn, S. Enhanced Visible Light Photocatalytic Activity of N and Ag Doped and Co-Doped TiO_2 Synthesized by Using an In-Situ Solvothermal Method for Gas Phase Ammonia Removal. *Catalysts* **2020**, *10*, 18, doi:10.3390/catal10020251.
165. Chauhan, N.; Singh, V.; Kumar, S.; Sirohi, K. Preparation of palladium, silver, and nitrogen co-doped mesoporous titanium dioxide nanoparticles to investigate their photocatalytic action. *Mater. Res. Express* **2019**, *6*, 13, doi:10.1088/2053-1591/ab50a7.
166. Osin, O.A.; Yu, T.Y.; Cai, X.M.; Jiang, Y.; Peng, G.T.; Cheng, X.M.; Li, R.B.; Qin, Y.; Lin, S.J. Photocatalytic Degradation of 4-Nitrophenol by C, N-TiO_2: Degradation Efficiency vs. Embryonic Toxicity of the Resulting Compounds. *Front. Chem.* **2018**, *6*, 9, doi:10.3389/fchem.2018.00192.
167. Zhao, Z.Y.; Feng, M.C.; Peng, Z.J.; Huang, H.W.; Guo, Z.H.; Li, Z.H. Molten-salt fabrication of (N,F)-codoped single-crystal-like titania with high exposure of (001) crystal facet for highly efficient degradation of methylene blue under visible light irradiation. *J. Mater. Res.* **2018**, *33*, 1411–1421, doi:10.1557/jmr.2018.106.
168. Wang, P.S.; Qi, C.X.; Wen, P.C.; Hao, L.Y.; Xu, X.; Agathopoulos, S. Synthesis of Si, N co-Doped Nano-Sized TiO_2 with High Thermal Stability and Photocatalytic Activity by Mechanochemical Method. *Nanomaterials* **2018**, *8*, 12, doi:10.3390/nano8050294.
169. Zhang, J.Q.; Xing, Z.P.; Cui, J.Y.; Li, Z.Z.; Tan, S.Y.; Yin, J.W.; Zou, J.L.; Zhu, Q.; Zhou, W. C,N co-doped porous TiO_2 hollow sphere visible light photocatalysts for efficient removal of highly toxic phenolic pollutants. *Dalton Trans.* **2018**, *47*, 4877–4884, doi:10.1039/c8dt00262b.
170. Singh, I.; Birajdar, B. Effective La-Na Co-Doped TiO_2 Nano-Particles for Dye Adsorption: Synthesis, Characterization and Study on Adsorption Kinetics. *Nanomaterials* **2019**, *9*, 15, doi:10.3390/nano9030400.
171. Li, Y.F.; Xu, D.H.; Oh, J.I.; Shen, W.; Li, X.; Yu, Y. Mechanistic Study of Codoped Titania with Nonmetal and Metal Ions: A Case of C plus Mo Codoped TiO_2. *ACS Catal.* **2012**, *2*, 391–398, doi:10.1021/cs2006668.

172. Garg, A.; Singhania, T.; Singh, A.; Sharma, S.; Rani, S.; Neogy, A.; Yadav, S.R.; Sangal, V.K.; Garg, N. Photocatalytic Degradation of Bisphenol-A using N, Co Codoped TiO_2 Catalyst under Solar Light. *Sci. Rep.* **2019**, *9*, 13, doi:10.1038/s41598-018-38358-w.
173. Wang, F.; Ma, Z.Z.; Ban, P.P.; Xu, X.H. C, N and S codoped rutile TiO_2 nanorods for enhanced visible-light photocatalytic activity. *Mater. Lett.* **2017**, *195*, 143–146, doi:10.1016/j.matlet.2017.02.113.
174. Wang, M.G.; Han, J.; Hu, Y.M.; Guo, R. Mesoporous C, N-codoped TiO_2 hybrid shells with enhanced visible light photocatalytic performance. *RSC Adv.* **2017**, *7*, 15513–15520, doi:10.1039/c7ra00985b.
175. Modanlu, S.; Shafiekhani, A. Synthesis of pure and C/S/N co-doped Titania on Al mesh and their photocatalytic usage in Benzene degradation. *Sci. Rep.* **2019**, *9*, 9, doi:10.1038/s41598-019-53189-z.
176. Zeng, X.L.; Sun, X.Z.; Yu, Y.S.; Wang, H.Y.; Wang, Y. Photocatalytic degradation of flumequine with B/N codoped TiO_2 catalyst: Kinetics, main active species, intermediates and pathways. *Chem. Eng. J.* **2019**, *378*, 10, doi:10.1016/j.cej.2019.122226.
177. Humayun, M.; Raziq, F.; Khan, A.; Luo, W. Modification strategies of TiO_2 for potential applications in photocatalysis: acritical review. *Green Chem. Lett. Rev.* **2018**, *11*, 86–102, doi:10.1080/17518253.2018.1440324.
178. Zhu, K.; Neale, N.R.; Miedaner, A.; Frank, A.J. Enhanced charge-collection efficiencies and light scattering in dye-sensitized solar cells using oriented TiO_2 nanotubes arrays. *Nano Lett.* **2007**, *7*, 69–74, doi:10.1021/nl062000o.
179. Zangeneh, H.; Zinatizadeh, A.A.L.; Habibi, M.; Akia, M.; Isa, M.H. Photocatalytic oxidation of organic dyes and pollutants in wastewater using different modified titanium dioxides: A comparative review. *J. Ind. Eng. Chem.* **2015**, *26*, 1–36, doi:10.1016/j.jiec.2014.10.043.
180. Toumazatou, A.; Arfanis, M.K.; Pantazopoulos, P.A.; Kontos, A.G.; Falaras, P.; Stefanou, N.; Likodimos, V. Slow-photon enhancement of dye sensitized TiO_2 photocatalysis. *Mater. Lett.* **2017**, *197*, 123–126, doi:10.1016/j.matlet.2017.03.128.
181. Diaz-Angulo, J.; Lara-Ramos, J.; Mueses, M.; Hernandez-Ramirez, A.; Li Puma, G.; Machuca-Martinez, F. Enhancement of the oxidative removal of diclofenac and of the TiO_2 rate of photon absorption in dye-sensitized solar pilot scale CPC photocatalytic reactors. *Chem. Eng. J.* **2020**, *381*, 12, doi:10.1016/j.cej.2019.122520.
182. Park, H.; Park, Y.; Kim, W.; Choi, W. Surface modification of TiO_2 photocatalyst for environmental applications. *J. Photochem. Photobiol. C Photochem. Rev.* **2013**, *15*, 1–20, doi:10.1016/j.jphotochemrev.2012.10.001.
183. Choi, S.K.; Yang, H.S.; Kim, J.H.; Park, H. Organic dye-sensitized TiO_2 as a versatile photocatalyst for solar hydrogen and environmental remediation. *Appl. Catal. B* **2012**, *121*, 206–213, doi:10.1016/j.apcatb.2012.04.011.
184. Dong, S.Y.; Feng, J.L.; Fan, M.H.; Pi, Y.Q.; Hu, L.M.; Han, X.; Liu, M.L.; Sun, J.Y.; Sun, J.H. Recent developments in heterogeneous photocatalytic water treatment using visible light-responsive photocatalysts: a review. *RSC Adv.* **2015**, *5*, 14610–14630, doi:10.1039/c4ra13734e.
185. Diaz-Angulo, J.; Gomez-Bonilla, I.; Jimenez-Tohapanta, C.; Mueses, M.; Pinzon, M.; Machuca-Martinez, F. Visible-light activation of TiO_2 by dye-sensitization for degradation of pharmaceutical compounds. *Photochem. Photobiol. Sci.* **2019**, *18*, 897–904, doi:10.1039/c8pp00270c.
186. Yun, E.T.; Yoo, H.Y.; Kim, W.; Kim, H.E.; Kang, G.; Lee, H.; Lee, S.; Park, T.; Lee, C.; Kim, J.H.; et al. Visible-light-induced activation of periodate that mimics dye-sensitization of TiO_2: Simultaneous decolorization of dyes and production of oxidizing radicals. *Appl. Catal. B* **2017**, *203*, 475–484, doi:10.1016/j.apcatb.2016.10.029.
187. Sengupta, D.; Das, P.; Mondal, B.; Mukherjee, K. Effects of doping, morphology and film-thickness of photo-anode materials for dye sensitized solar cell application - A review. *Renew. Sust. Energ. Rev.* **2016**, *60*, 356–376, doi:10.1016/j.rser.2016.01.104.
188. Ahmad, I.; Kan, C.W. Visible-Light-Driven, Dye-Sensitized TiO2 Photo-Catalyst for Self-Cleaning Cotton Fabrics. *Coatings* **2017**, *7*, 13, doi:10.3390/coatings7110192.
189. Murcia, J.J.; Avila-Martinez, E.G.; Rojas, H.; Cubillos, J.; Ivanova, S.; Penkova, A.; Laguna, O.H. Powder and Nanotubes Titania Modified by Dye Sensitization as Photocatalysts for the Organic Pollutants Elimination. *Nanomaterials* **2019**, *9*, 11, doi:10.3390/nano9040517.
190. Guo, G.Q.; Guo, H.Y.; Wang, F.; France, L.J.; Yang, W.X.; Mei, Z.H.; Yu, Y.H. Dye-sensitized TiO_2@SBA-15 composites: Preparation and their application in photocatalytic desulfurization. *Green Energy Environ.* **2020**, *5*, 114–120, doi:10.1016/j.gee.2019.11.005.

191. Xu, T.Z.; Zhao, H.C.; Zheng, H.; Zhang, P.Y. Atomically Pt implanted nanoporous TiO_2 film for photocatalytic degradation of trace organic pollutants in water. *Chem. Eng. J.* **2020**, *385*.
192. Lu, L.L.; Shan, R.; Shi, Y.Y.; Wang, S.X.; Yuan, H.R. A novel TiO_2/biochar composite catalysts for photocatalytic degradation of methyl orange. *Chemosphere* **2019**, *222*, 391–398, doi:10.1016/j.chemosphere.2019.01.132.
193. Ismael, M. Enhanced photocatalytic hydrogen production and degradation of organic pollutants from Fe (III) doped TiO_2 nanoparticles. *J. Environ. Chem. Eng.* **2020**, *8*, 9, doi:10.1016/j.jece.2020.103676.
194. Xu, J.J.; Chen, Y.F.; Dong, Z.Y.; Peng, Y.N.; Yue, S.T.; Huang, H. Strong effect of multi-electron oxygen reduction reaction on photocatalysis through the promotion of interfacial charge transfer. *Appl. Catal. B* **2019**, *252*, 41–46, doi:10.1016/j.apcatb.2019.03.075.
195. Singh, K.; Harish, S.; Archana, J.; Navaneethan, M.; Shimomura, M.; Hayakawa, Y. Investigation of Gd-doped mesoporous TiO_2 spheres for environmental remediation and energy applications. *Appl. Surf. Sci.* **2019**, *489*, 883–892, doi:10.1016/j.apsusc.2019.05.253.
196. Zhang, J.L.; Pang, Z.Y.; Sun, Q.; Chen, X.; Zhu, Y.A.; Li, M.J.; Wang, J.D.; Qiu, H.; Li, X.Q.; Li, Y.G.; et al. TiO_2 nanotube array modified with polypyrrole for efficient photoelectrocatalytic decolorization of methylene blue. *J. Alloy. Compd.* **2020**, *820*, 10, doi:10.1016/j.jallcom.2019.153128.
197. Singaram, B.; Jeyaram, J.; Rajendran, R.; Arumugam, P.; Varadharajan, K. Visible light photocatalytic activity of tungsten and fluorine codoped TiO_2 nanoparticle for an efficient dye degradation. *Ionics* **2019**, *25*, 773–784, doi:10.1007/s11581-018-2628-x.
198. Janbandhu, S.Y.; Joshi, A.; Munishwar, S.R.; Gedam, R.S. CdS/TiO_2 heterojunction in glass matrix: Synthesis, characterization, and application as an improved photocatalyst. *Appl. Surf. Sci.* **2019**, *497*, 11, doi:10.1016/j.apsusc.2019.143758.
199. Liu, C.Q.; Li, X.; Wu, Y.T.; Zhang, L.Y.; Chang, X.J.; Yuan, X.X.; Wang, X.F. Fabrication of multilayer porous structured TiO2-$ZrTiO_4$-SiO_2 heterostructure towards enhanced photo-degradation activities. *Ceram. Int.* **2020**, *46*, 476–486, doi:10.1016/j.ceramint.2019.08.285.
200. Wang, R.; Shen, J.; Zhang, W.J.; Liu, Q.Q.; Zhang, M.Y.; Zulfiqar; Tang, H. Build-in electric field induced step-scheme TiO_2/$W_{18}O_{49}$ heterojunction for enhanced photocatalytic activity under visible-light irradiation. *Ceram. Int.* **2020**, *46*, 23–30, doi:10.1016/j.ceramint.2019.08.226.
201. Thanh, T.L.T.; Thi, L.N.; Dinh, T.T.; Van, N.N. Enhanced Photocatalytic Degradation of Rhodamine B Using C/Fe Co-Doped Titanium Dioxide Coated on Activated Carbon. *J. Chem.* **2019**, 10.1155/2019/2949316, 8, doi:10.1155/2019/2949316.
202. Kumar, A.; Khan, M.; He, J.H.; Lo, I.M.C. Visible-light-driven magnetically recyclable terephthalic acid functionalized g-C_3N_4/TiO_2 heterojunction nanophotocatalyst for enhanced degradation of PPCPs. *Appl. Catal. B* **2020**, *270*, 12, doi:10.1016/j.apcatb.2020.118898.
203. Chen, M.; Wang, H.H.; Chen, X.Y.; Wang, F.; Qin, X.X.; Zhang, C.B.; He, H. High-performance of Cu-TiO_2 for photocatalytic oxidation of formaldehyde under visible light and the mechanism study. *Chem. Eng. J.* **2020**, *390*, 8, doi:10.1016/j.cej.2020.124481.
204. He, L.; Dong, Y.N.; Zheng, Y.N.; Jia, Q.M.; Shan, S.Y.; Zhang, Y.Q. A novel magnetic MIL-101(Fe)/TiO_2 composite for photo degradation of tetracycline under solar light. *J. Hazard. Mater.* **2019**, *361*, 85–94, doi:10.1016/j.jhazmat.2018.08.079.
205. Namshah, K.S.; Mohamed, R.M. WO_3-TiO_2 nanocomposites for paracetamol degradation under visible light. *Appl. Nanosci.* **2018**, *8*, 2021–2030, doi:10.1007/s13204-018-0888-4.
206. Shi, Z.; Xu, P.F.; Shen, X.F.; Zhang, Y.; Luo, L.; Duoerkun, G.; Zhang, L.S. TiO_2/MoS_2 heterojunctions-decorated carbon fibers with broad-spectrum response as weaveable photocatalyst/photoelectrode. *Mater. Res. Bull.* **2019**, *112*, 354–362, doi:10.1016/j.materresbull.2019.01.005.
207. Djouadi, L.; Khalaf, H.; Boukhatem, H.; Boutoumi, H.; Kezzime, A.; Santaballa, J.A.; Canle, M. Degradation of aqueous ketoprofen by heterogeneous photocatalysis using Bi_2S_3/TiO_2-Montmorillonite nanocomposites under simulated solar irradiation. *Appl. Clay Sci.* **2018**, *166*, 27–37, doi:10.1016/j.clay.2018.09.008.
208. Leal, J.F.; Cruz, S.M.A.; Almeida, B.T.A.; Esteves, V.I.; Marques, P.; Santos, E.B.H. TiO_2-rGO nanocomposite as an efficient catalyst to photodegrade formalin in aquaculture's waters, under solar light. *Environ. Sci. Wat. Res. Technol.* **2020**, *6*, 1018–1027, doi:10.1039/c9ew00950g.
209. Morones-Esquivel, M.M.; Nunez-Nunez, C.M.; Gonzalez-Burciaga, L.A.; Hernandez-Mendoza, J.L.; Osorio-Revilla, G.I.; Proal-Najera, J.B. Kinetics and statistical approach for 2,5-dichlorophenol degradation

in short reaction times by solar TiO_2/glass photocatalysis. *Rev. Mex. Ing. Quim.* **2020**, *19*, 555–568, doi:10.24275/rmiq/Cat732.

210. Borzyszkowska, A.F.; Pieczynska, A.; Ofiarska, A.; Lisowski, W.; Nikiforow, K.; Siedlecka, E.M. Photocatalytic degradation of 5-fluorouracil in an aqueous environment via Bi-B co-doped TiO_2 under artificial sunlight. *Int. J. Environ. Sci. Technol.* **2020**, *17*, 2163–2176, doi:10.1007/s13762-019-02604-z.
211. Tbessi, I.; Benito, M.; Molins, E.; Llorca, J.; Touati, A.; Sayadi, S.; Najjar, W. Effect of Ce and Mn co-doping on photocatalytic performance of sol-gel TiO_2. *Solid State Sci.* **2019**, *88*, 20–28, doi:10.1016/j.solidstatesciences.2018.12.004.
212. Saqlain, S.; Cha, B.J.; Kim, S.Y.; Ahn, T.K.; Park, C.; Oh, J.M.; Jeong, E.C.; Seo, H.O.; Kim, Y.D. Visible light-responsive Fe-loaded TiO_2 photocatalysts for total oxidation of acetaldehyde: Fundamental studies towards large-scale production and applications. *Appl. Surf. Sci.* **2020**, *505*, 9, doi:10.1016/j.apsusc.2019.144160.
213. Cherni, D.; Moussa, N.; Nsib, M.F.; Olivo, A.; Signoretto, M.; Prati, L.; Villa, A. Photocatalytic degradation of ethylbenzene in gas phase over N or NF doped TiO_2 catalysts. *J. Mater. Sci. Mater. Electron.* **2019**, *30*, 18919–18926, doi:10.1007/s10854-019-02248-2.
214. Jaleh, B.; Rouzbahani, M.G.; Abedi, K.; Azizian, S.; Ebrahimi, H.; Nasrollahzadeh, M.; Varma, R.S. Photocatalytic decomposition of VOCs by AC-TiO_2 and EG-TiO_2 nanocomposites. *Clean Technol. Environ. Policy* **2019**, *21*, 1259–1268, doi:10.1007/s10098-019-01702-3.
215. Kim, J.; Lee, B.K. Enhanced photocatalytic decomposition of VOCs by visible-driven photocatalyst combined Cu-TiO_2 and activated carbon fiber. *Process Saf. Environ. Protect.* **2018**, *119*, 164–171, doi:10.1016/j.psep.2018.07.026.
216. Belet, A.; Wolfs, C.; Mahy, J.G.; Poelman, D.; Vreuls, C.; Gillard, N.; Lambert, S.D. Sol-gel Syntheses of Photocatalysts for the Removal of Pharmaceutical Products in Water. *Nanomater. Basel* **2019**, *9*.
217. Saif, M.; Aboul-Fotouh, S.M.K.; El-Molla, S.A.; Ibrahim, M.M.; Ismail, L.F.M. Evaluation of the photocatalytic activity of Ln(3+)-TiO_2 nanomaterial using fluorescence technique for real wastewater treatment. *Spectroc. Acta Pt. A Molec. Biomolec. Spectr.* **2014**, *128*, 153–162, doi:10.1016/j.saa.2014.02.031.
218. Lima, K.V.; Emídio, E.S.; Pupo Nogueira, R.F.; Vasconcelos, N.d.S.L.; Araújo, A.B. Application of a stable Ag/TiO_2 film in the simultaneous photodegradation of hormones. *J. of Chem. Technol. Biotechnol.* **2020** , *8*, doi:10.1002/jctb.6258.
219. Peng, X.M.; Wang, M.; Hu, F.P.; Qiu, F.X.; Dai, H.L.; Cao, Z. Facile fabrication of hollow biochar carbon-doped TiO_2/CuO composites for the photocatalytic degradation of ammonia nitrogen from aqueous solution. *J. Alloy. Compd.* **2019**, *770*, 1055–1063, doi:10.1016/j.jallcom.2018.08.207.
220. Li, S.M.; Tan, J.; Jiang, Z.J.; Wang, J.; Li, Z.Q. MOF-derived bimetallic Fe-Ni-P nanotubes with tunable compositions for dye-sensitized photocatalytic H_2 and O_2 production. *Chem. Eng. J.* **2020**, *384*.
221. Saad, A.M.; Abukhadra, M.R.; Abdel-Kader Ahmed, S.; Elzanaty, A.M.; Mady, A.H.; Betiha, M.A.; Shim, J.-J.; Rabie, A.M. Photocatalytic degradation of malachite green dye using chitosan supported ZnO and Ce-ZnO nano-flowers under visible light. *J. Environ. Manag.* **2020**, *258*, 110043, doi:10.1016/j.jenvman.2019.110043.
222. Espino-Estevez, M.R.; Fernandez-Rodriguez, C.; Gonzalez-Diaz, O.M.; Arana, J.; Espinos, J.P.; Ortega-Mendez, J.A.; Dona-Rodriguez, J.M. Effect of TiO_2-Pd and TiO_2-Ag on the photocatalytic oxidation of diclofenac, isoproturon and phenol. *Chem. Eng. J.* **2016**, *298*, 82–95, doi:10.1016/j.cej.2016.04.016.
223. Xu, H.F.; Li, G.; Liu, N.; Zhu, K.R.; Zhu, G.; Jin, S.W. Ag @ hierarchical TiO_2 core-shell nanostructures for enhanced photocatalysis. *Mater. Lett.* **2015**, *142*, 324–327, doi:10.1016/j.matlet.2014.12.016.
224. Ji, L.J.; Liu, X.; Xu, T.; Gong, M.D.; Zhou, S. Preparation and photocatalytic properties of carbon/carbon-doped TiO_2 double-layer hollow microspheres. *J. Sol Gel Sci. Technol.* **2020**, *93*, 380–390, doi:10.1007/s10971-019-05176-z.
225. Fu, Z.T.; Zhang, S.; Fu, Z.X. Preparation of Multicycle GO/TiO_2 Composite Photocatalyst and Study on Degradation of Methylene Blue Synthetic Wastewater. *Appl. Sci. Basel* **2019**, *9*, 12, doi:10.3390/app9163282.
226. He, X.; Wang, X.C.; Cheng, B.Z.; Cao, S.; Zhou, J.F. Application of Mn-doped Mesoporous TiO_2 in Tannery Wastewater Treatment. *J. Soc. Leather Technol. Chem.* **2019**, *103*, 318–322.
227. Bordes, M.C.; Vicent, M.; Moreno, R.; Garcia-Montano, J.; Serra, A.; Sanchez, E. Application of plasma-sprayed TiO_2 coatings for industrial (tannery) wastewater treatment. *Ceram Int.* **2015**, *41*, 14468–14474.
228. Kim, K.H.; Kabir, E.; Jahan, S.A. Exposure to pesticides and the associated human health effects. *Sci. Total Environ.* **2017**, *575*, 525–535.

229. Fiorenza, R.; Di Mauro, A.; Cantarella, M.; Iaria, C.; Scalisi, E.M.; Brundo, M.V.; Gulino, A.; Spitaleri, L.; Nicotra, G.; Dattilo, S.; et al. Preferential removal of pesticides from water by molecular imprinting on TiO_2 photocatalysts. *Chem. Eng. J.* **2020**, *379*.
230. Abdennouri, M.; Baalala, M.; Galadi, A.; El Makhfouk, M.; Bensitel, M.; Nohair, K.; Sadiq, M.; Boussaoud, A.; Barka, N. Photocatalytic degradation of pesticides by titanium dioxide and titanium pillared purified clays. *Arab. J. Chem.* **2016**, *9*, S313-S318, doi:10.1016/j.arabjc.2011.04.005.
231. Nasseh, N.; Taghavi, L.; Barikbin, B.; Nasseri, M.A. Synthesis and characterizations of a novel $FeNi_3/SiO_2/CuS$ magnetic nanocomposite for photocatalytic degradation of tetracycline in simulated wastewater. *J Clean Prod.* **2018**, *179*, 42–54.
232. Oliveira, C.P.M.d.; Viana, M.M.; Amaral, M.C.S. Coupling photocatalytic degradation using a green TiO_2 catalyst to membrane bioreactor for petroleum refinery wastewater reclamation. *Comp. Immunol. Microbiol. Infect. Dis.* **2019**, *68*, 101403, doi:10.1016/j.cimid.2019.101403.
233. Ani, I.J.; Akpan, U.G.; Olutoye, M.A.; Hameed, B.H. Photocatalytic degradation of pollutants in petroleum refinery wastewater by TiO_2- and ZnO-based photocatalysts: Recent development. *J. Clean Prod.* **2018**, *205*, 930–954, doi:10.1016/j.jclepro.2018.08.189.
234. Shivaraju, H.P.; Muzakkira, N.; Shahmoradi, B. Photocatalytic treatment of oil and grease spills in wastewater using coated N-doped TiO_2 polyscales under sunlight as an alternative driving energy. *Int. J. Environ. Sci. Technol.* **2016**, *13*, 2293–2302, doi:10.1007/s13762-016-1038-8.
235. Andronic, L.; Isac, L.; Miralles-Cuevas, S.; Visa, M.; Oller, I.; Duta, A.; Malato, S. Pilot-plant evaluation of TiO_2 and TiO_2-based hybrid photocatalysts for solar treatment of polluted water. *J. Hazard Mater.* **2016**, *320*, 469–478.
236. Solis-Casados, D.A.; Escobar-Alarcon, L.; Gomez-Olivan, L.M.; Haro-Poniatowski, E.; Klimova, T. Photodegradation of pharmaceutical drugs using Sn-modified TiO_2 powders under visible light irradiation. *Fuel* **2017**, *198*, 3–10, doi:10.1016/j.fuel.2017.01.059.
237. Malakootian, M.; Olama, N.; Malakootian, M.; Nasiri, A. Photocatalytic degradation of metronidazole from aquatic solution by TiO_2-doped Fe^{3+} nano-photocatalyst. *Int. J. Environ. Sci. Technol.* **2019**, *16*, 4275–4284, doi:10.1007/s13762-018-1836-2.
238. Lacerda, J.A.S.; Macedo, A.M.; Teixeira, R.I.; Simoes, G.; Ribeiro, E.S.; Forero, J.S.B.; Correa, R.J. TiO_2 Decorated Sand Grains for Photodegradation of Pollutants: Methylene Blue and Ciprofloxacin Study. *J. Braz. Chem. Soc.* **2020**, *31*, 201–210, doi:10.21577/0103-5053.20190129.
239. Hou, C.T.; Xie, J.Q.; Yang, H.L.; Chen, S.M.; Liu, H.L. Preparation of $Cu2O@TiOF_2/TiO_2$ and its photocatalytic degradation of tetracycline hydrochloride wastewater. *RSC Adv.* **2019**, *9*, 37911–37918, doi:10.1039/c9ra07999h.
240. Li, S.P.; Chang, L.B.; Peng, J.H.; Gao, J.Z.; Lu, J.B.; Zhang, F.C.; Zhu, G.Q.; Hojamberdiev, M. Bi-0 nanoparticle loaded on Bi^{3+}-doped $ZnWO_4$ nanorods with oxygen vacancies for enhanced photocatalytic NO removal. *J. Alloy. Compd.* **2020**, *818*, 9, doi:10.1016/j.jallcom.2019.152837.
241. Rao, F.; Zhu, G.Q.; Hojamberdiev, M.; Zhang, W.B.; Li, S.P.; Gao, J.Z.; Zhang, F.C.; Huang, Y.H.; Huang, Y. Uniform Zn^{2+}-Doped BiOI Microspheres Assembled by Ultrathin Nanosheets with Tunable Oxygen Vacancies for Super-Stable Removal of NO. *J. Phys. Chem. C* **2019**, *123*, 16268–16280.
242. Zhang, G.X.; Sun, Z.M.; Duan, Y.W.; Ma, R.X.; Zheng, S.L. Synthesis of nano-TiO_2/diatomite composite and its photocatalytic degradation of gaseous formaldehyde. *Appl. Surf. Sci.* **2017**, *412*, 105–112, doi:10.1016/j.apsusc.2017.03.198.
243. Qin, Z.B.; Zhang, W.T.; Qian, G.P.; Wu, X.L.; Li, Y.J.M.R.I. The effects of different ways of adding nano-TiO_2 to concrete on the degradation performance of NO_2. *Mater. Res. Innov.* **2015**, *19*, S10-S148.
244. Zhang, J.H.; Hu, Y.; Qin, J.X.; Yang, Z.X.; Fu, M.L. TiO_2-UiO-66-NH_2 nanocomposites as efficient photocatalysts for the oxidation of VOCs. *Chem. Eng. J.* **2020**, *385*.
245. Wang, X.G.; Sun, M.H.; Murugananthan, M.; Zhang, Y.R.; Zhang, L.Z. Electrochemically self-doped WO_3/TiO_2 nanotubes for photocatalytic degradation of volatile organic compounds. *Appl. Catal. B* **2020**, *260*.
246. Lai, M.; Zhao, J.; Chen, Q.C.; Feng, S.J.; Bai, Y.J.; Li, Y.X.; Wang, C.Y. Photocatalytic toluene degradation over Bi-decorated TiO_2: Promoted O_2 supply to catalyst's surface by metallic Bi. *Catal. Today* **2019**, *335*, 372–380, doi:10.1016/j.cattod.2018.12.045.
247. Rao, Z.P.; Xie, X.F.; Wang, X.; Mahmood, A.; Tong, S.R.; Ge, M.F.; Sun, J. Defect Chemistry of Er^{3+}-Doped TiO_2 and Its Photocatalytic Activity for the Degradation of Flowing Gas-Phase VOCs. *J. Phys. Chem. C* **2019**, *123*, 12321–12334, doi:10.1021/acs.jpcc.9b02093.

248. Ali, N.; Bilal, M.; Khan, A.; Ali, F.; Iqbal, H.M.N. Effective exploitation of anionic, nonionic, and nanoparticle-stabilized surfactant foams for petroleum hydrocarbon contaminated soil remediation. *Sci. Total Environ.* **2020**, *704*.
249. Peikam, E.N.; Jalali, M. Application of three nanoparticles (Al_2O_3, SiO_2 and TiO_2) for metal-contaminated soil remediation (measuring and modeling). *Int. J. Environ. Sci. Technol.* **2019**, *16*, 7207–7220.
250. Wang, L.; Li, X.; Tsang, D.C.W.; Jin, F.; Hou, D. Green remediation of Cd and Hg contaminated soil using humic acid modified montmorillonite: Immobilization performance under accelerated ageing conditions. *J. Hazard Mater.* **2020**, *387*, 122005, doi:10.1016/j.jhazmat.2019.122005.
251. Khalid, S.; Shahid, M.; Murtaza, B.; Bibi, I.; Natasha; Asif Naeem, M.; Niazi, N.K. A critical review of different factors governing the fate of pesticides in soil under biochar application. *Sci. Total Environ.* **2020**, *711*, 134645, doi:10.1016/j.scitotenv.2019.134645.
252. Eker, G.; Hatipoglu, M. Effect of UV wavelength, temperature and photocatalyst on the removal of PAHs from industrial soil with photodegradation applications. *Environ. Technol.* **2019**, *40*, 3793–3803, doi:10.1080/09593330.2018.1491635.
253. Rachna; Rani, M.; Shanker, U. Degradation of tricyclic polyaromatic hydrocarbons in water, soil and river sediment with a novel TiO_2 based heterogeneous nanocomposite. *J. Environ. Manage.* **2019**, *248*.
254. Zyoud, A.; Ateeq, M.; Helal, M.H.; Zyoud, S.H.; Hilal, H.S. Photocatalytic degradation of phenazopyridine contaminant in soil with direct solar light. *Environ. Technol.* **2019**, *40*, 2928–2939, doi:10.1080/09593330.2018.1459873.
255. Xu, Q.; Huang, Z.; Ji, S.T.; Zhou, J.; Shi, R.Z.; Shi, W.Y. Cu_2O nanoparticles grafting onto PLA fibers via electron beam irradiation: bifunctional composite fibers with enhanced photocatalytic of organic pollutants in aqueous and soil systems. *J. Radioanal Nucl. Chem.* **2019**.
256. Theerakarunwong, C.D.; Phanichphant, S. Visible-Light-Induced Photocatalytic Degradation of PAH-Contaminated Soil and Their Pathways by Fe-Doped TiO_2 Nanocatalyst. *Water Air Soil Poll.* **2018**, *229*, 11, doi:10.1007/s11270-018-3951-6.
257. Kuang, X.; Shao, J.; Peng, L.; Song, H.; Wei, X.; Luo, S.; Gu, J.-D. Nano-TiO_2 enhances the adsorption of Cd(II) on biological soil crusts under mildly acidic conditions. *J. Contam. Hydrol.* **2020**, *229*, 103583, doi:10.1016/j.jconhyd.2019.103583.
258. Yang, Y.; Javed, H.; Zhang, D.N.; Li, D.Y.; Kamath, R.; McVey, K.; Sra, K.; Alvarez, P.J.J. Merits and limitations of TiO_2-based photocatalytic pretreatment of soils impacted by crude oil for expediting bioremediation. *Front Chem. Sci. Eng.* **2017**, *11*, 387–394, doi: 10.1007/s11705-017-1657-8